Approximating meteoric ^{10}Be using the concentration of acid-extractable grain coatings: a case study tracing erosion depth on Dominica, Lesser Antilles

By Kira Tomenchok

Undergraduate Honors Thesis in Geology

May 2018

Advisor: David Harbor

Washington and Lee University

Table of Contents

Abstract

Surface process studies on Dominica have emphasized landslide research in order to improve hazard mitigation, but a deficit exists in understanding the general geomorphic processes. The goal of this study is to characterize erosional processes, in addition to landslides, using sediment-fingerprinting techniques. Meteoric ^{10}Be is an accepted fingerprinting tool used to identify sediment sources and infer erosional processes. Due the analytical cost of $^{10}Be_m$, we test the validity of the concentration of grain coatings as a proxy for $^{10}Be_m$ in a Caribbean setting. We sampled detrital sediment in two sizes, <63 and 250-850 μm, from the outlets of Dominica's 20 largest watersheds. A strong positive correlation exists between acid-extractable grain coating concentrations from <63 μm sediment and $^{10}Be_m$, but a weak correlation exists between grain coating concentrations from 250-850 μm sediments and $^{10}Be_m$. Acid-extractable Fe, Al and Mn, concentrations are selected as the total concentration of grain coatings. With this technique, selected elements are site-dependent; the elements in our study vary with elements selected in Singleton et al. (2017) and Greene (2016). This research affirmed the viability of grain coating concentrations leached from fine-grained sediment as proxy for $^{10}Be_m$. Transport to the outlet likely affects coating concentrations on coarse-grained sediment more than fine-grained sediment through processes such as abrasion, decreasing the viability of using coarse-sample grain coatings. A strong inverse relationship exists between fine-sample grain coatings and landslide density, affirming that changes of erosional processes are represented in the outlet sediment. Furthermore, watershed characteristics account for varying erosional processes between watersheds. Individual precipitation events and slope show the strongest correlation with landslide activity and land use and geology show weak but positive relationships with landslide activity.

Introduction

Dominica, an island in the Caribbean, experiences the harmful social and economic effects of landslides (De Graff et al., 1989). Steep topography, geology and heavy precipitation create an environment conducive to damaging erosional processes. Intense rainfall events, frequent in Dominica, are the principle mechanism for inducing landslides (De Graff et al., 1989). Tropical Storm Erika in 2015 and most recently Hurricane Maria in September 2017 devastated the island and resulted in major landslides and flooding (van Westen et al., 2018). Between 1925 and 2015, landslides were responsible for the deaths of 35 Dominicans (van Westen, 2016). In addition to fatalities and injuries, landslides require infrastructure reparation leading to a serious economic impact. Landslides regularly damage roads, structures and pipelines for hydroelectric and water systems (De Graff et al., 1989). De Graff et al. (1989) calculated that 30 years ago road repair, clearing debris and other associated landslide repairs resulted in an average annual cost of $121,000 EC.

Due to the immediate and prominent impact of landslides, several studies have characterized and quantified landslides on Dominica. De Graff (1987) developed the first landslide hazard map of Dominica and De Graff (1990) revisited and improved his 1987 study. Detailed landslide susceptibility studies further assessed the landscape indicators that induce landsliding. Andereck (2007) performed multiple logistic regressions to calculate local landslide probability maps, assessing factors of soil type, land cover/ land use, slope, aspect, and distance to nearest road. Van Westen (2016) performed a bi-variate statistical analysis to generate a national-scale landslide susceptibility map, assessing factors of topography, drainage, geology, soil and land cover. Other than landslides, erosional processes in the Caribbean are relatively

understudied (Portenga and Bierman, 2011). Therefore, general geomorphic processes can be studied based on the characteristics assessed in landslide susceptibility studies.

This study uses sediment tracers to gain a larger scope of the geomorphic processes on Dominica. Sediment tracing is important to understanding the correlation between surface processes and factors such as climate, tectonics and human activity (Singleton et al., 2017). We assume the geochemical signatures of detrital sediment is representative of an entire upstream basin. The tracer of our focus is meteoric beryllium-10, which is important in determining the depth of erosion in a watershed. Our study focuses on developing the concentration of acid-extractable grain coatings as a proxy for meteoric ^{10}Be.

The purpose of this paper is twofold. We intend to interpret the erosional processes of an entire upstream basin using the elemental concentration of grain coatings on detrital sediment (Greene, 2016). We will develop a baseline understanding of the erosional processes within each watershed on Dominica, inferring landslide, riverbanks/scarps or surface erosion. Furthermore, we seek to determine the validity of using the elemental concentration of grain coatings as a proxy for meteoric ^{10}Be in detrital sediment. With catchment sediment-source identification, our goal is to better assess sediment dynamics on Dominica and ultimately improve hazard mitigation.

Study Area

Dominica, a 750 km^2 island, is located centrally in the Lesser Antilles arc in the eastern Caribbean (Fig. 1). The island arc formed from the subduction of the North American Plate beneath the Caribbean Plate (Lindsay et al., 2003). Dominica sits above a segmentation in the subduction slab; two slab segments with differences in subduction angle and subduction rate drive the high volcanism and steep topography on Dominica (Frey, 2016). With nine potentially

active volcanic centers, volcanic activity dominates the topography of the island. The highest peaks on Dominica are two dormant volcanoes, Morne Diablotins and Morne Trois Ptions, with peaks of 1335 m. and 1286 m., respectively. Abundant in hydrothermal activity, the island contains numerous hot springs and fumeroles, such as Champagne Beach, the Boiling lake and Valley of Desolation (Andereck, 2007). The geology is primarily volcanic including andesite, dacite, basalt, ignimbrites, and block and ash flows (Rouse et al., 1986; Frey, 2016). Ignimbrite deposits consist of pumice, rock and ash solidified during pyroclastic flows (Frey, 2016).

The climatic setting of Dominica is warm with heavy precipitation as a result of the northeast trade winds (De Graff et al., 1989; Andereck, 2007). Orographic effects cause a high annual rainfall, with the primary wet season occuring between June and December (Andereck, 2007). The windward side, interior highlands and leeward side experience an average annual precipitation of 3050 mm, 7620 mm, and 1270 mm, respectively (Andereck, 2007). Tropical storms and hurricanes are significant threats to Dominica. Between 1872 and 2014, Dominica experienced 31 tropical storms and 22 hurricanes (Westen, 2016).

Heavy precipitation, coupled with volcanic geology and steep topography, initiate frequent landslide activity on Dominica. The rapid weathering of bedrock under humid conditions creates weak regolith susceptible to mass wasting (De Graff et al., 1989). Heavy precipitation increases pore water pressure in weathered material, decreasing shear strength in soils (De Graff et al., 1989). In addition to rainfall, trigger mechanisms on Dominica include earthquakes, volcanic seismic swarms, and increased human activity. Development in cities, roads, deforestation and agricultural practices decrease soil stability and increase landslide susceptibility (van Westen, 2016). The majority of landslides occur on mountainous slopes, involving debris flows and debris slides. Less frequent landslides include rockslides and

rockfalls, which occur on bedrock escarpments, and slumps, which occur on human-disturbed slopes (De Graff et al., 1989).

Berryllium-10

Beryllilum-10 (^{10}Be) is a cosmogenic radionuclide (half-life of 1.39 million years) produced in two environments from O and N: meteoric and *in situ*. Meteoric ^{10}Be forms by the spallation of oxygen or nitrogen in the atmosphere (Graly et al., 2010) and *in situ* ^{10}Be forms within the mineral lattices of surface material (Willenbring, 2010). Our focus, meteoric ^{10}Be ($^{10}Be_m$) is a sediment tracer used to measure soil residence times, trace soil transport, quantify river sediment and dissolved fluxes (Willenbring, 2010). In the atmosphere $^{10}Be_m$ adheres to aerosols and is delivered to Earth's surface by precipitation or dry deposition (Graly et al., 2010). At the surface, $^{10}Be_m$ adheres to the upper few meters of soil and surface sediment (Willenbring, 2010). The longer half-life, when compared to other radioactive tracers, increases the time and depth in which $^{10}Be_m$ penetrates soils before decay (Graly et al., 2010; Reusser et al., 2010). Thus, $^{10}Be_m$ concentrations represent near surface residence time of sediment samples (Sosa Gonzalez et al., 2017). The concentration of $^{10}Be_m$ in detrital river sediments is an important metric in surface processes; specifically, $^{10}Be_m$ can be used to constrain the depth of sediment erosion (Reusser and Bierman, 2010) and the residence time of sediment (Sosa Gonzalez et al., 2017). Soils in slowly eroding landscapes tend to have higher concentrations of $^{10}Be_m$ due to a greater residence time and shallow erosion (Fig. 2). Low $^{10}Be_m$ concentrations are present in sediment sourced from rapidly eroding landscapes and from sediment sourced below the $^{10}Be_m$ accumulation zone (i.e. deeply penetrating gullies or deep-seated landslides (Fig. 2)) (Reusser and Bierman, 2010).

Concentration of Grain Coatings

While the technique is a proven method, $^{10}Be_m$ analyses are expensive and we are testing an alternative method. A strong, positive correlation exists between total $^{10}Be_m$ and acid-extractable grain coating concentrations, suggesting $^{10}Be_m$ is associated with weathering materials (Singleton et al., 2017; Greene, 2016). Acid extraction attacks crystalline and amorphous oxides/hydroxides (Greene, 2016), which make up the grain coatings to which Be adheres. Grain coatings form during podsolization, the process in which Fe^+, Al^+, and weathering products translocate through soil and form a thin film around grains in the B horizon (Birkeland, 1984). Be ions complex with organic matter and these organic Be complexes sorb to sediment by associating with existing grain coatings (Greene, 2016). The surfaces of weathering materials, such as oxides, hydroxides and clays, are reactive; Be atoms will adhere to these surfaces. Within 2:1 clay minerals, Be atoms adhere to the exchangeable sheet of water and cations. HCl acid-extractable grain coatings are primarily composed of Fe, Al, Ca, Mg, and Mn (Singleton et al., 2017; Greene, 2016) suggesting oxides, hydroxides and 2:1 clays are a significant portion of the grain coatings (Singleton et al., 2017). Due to the manner in which $^{10}Be_m$ adsorbs to grain coatings, the elemental concentration of grain coatings on detrital sediment serves as a proxy for $^{10}Be_m$ concentrations.

This study interprets the erosional processes of 20 watersheds on Dominica from sediment collection in the river outlets. The elemental concentrations of the acid-extractable grain coatings on detrital sediments are tested against $^{10}Be_m$ concentrations of selected watersheds to evaluate the proxy. We expect the geochemical signatures to characterize the erosional processes occurring within each basin (Fig. 3). Several assumptions underlie this technique. We assume the sediment sample at the outlet is homogenized and representative of

the entire upstream basin (Sosa Gonzalez et al., 2017). Moreover, we assume the sediment is well mixed and the concentration of analyte is steady over the time period of analysis (Sosa Gonzalez et al., 2017).

With the extensive landslide analysis that other studies have conducted, we can evaluate erosional processes using previously mapped landslides. By quantifying the concentration of grain coatings, we will determine the impact of landslides on the geochemical signature of river sediment. We hypothesize that watersheds with stabilizing landslide scars will have medium grain coating concentrations. Watersheds with river bank/scarp erosion or active landslides will have low grain coating concentrations. Watersheds with predominantly slow surface erosion will have high grain coating concentrations.

Methods

Field Work

We characterized watersheds on Dominica with a series of GIS and geochemical analysis. We mapped watersheds greater than 20 km^2 to locate the river outlets where we would collect detrital sediment (Fig. 4). In the field, we located the watershed outlets and collected fluvial sediment from 20 active river channels. At each site we performed the same sediment collection procedure. We used two different wet sieve sizes to collect <63 (fine-grained) and 250-850 (coarse-grained) μm sediment. With the <63 μm sieve, we collected the fine-grained sediment into 10 gallon buckets, pouring water and sediment through the sieve into the bucket. We collected coarse-grained sediment by sieving sediment through the 850 μm and 250 μm sieves, collecting sediment left behind in the 250 sieve into 2-3 gallon-sized bags. Concentration of HCl-extractable material depends on grain sizes, which are found in very fine grain sizes and coarse grain sizes (Sosa Gonzalez et al., 2017). When collecting sediment at a site, we spanned a

50 m radius to ensure a thorough collection of well mixed sediment (Sosa Gonzalez et al., 2017). We also avoided any tidal influence in the river (by sampling at least 100 m from the ocean) to confine sediment collected to the upstream watershed.

We sampled in July 2018 throughout a two week period, when it rained daily. In general, our sample sites were located near urban features such as roads and bridges (Fig. 5). Vegetated banks were common at each location but bank steepness varied. Water depth ranged from 10 cm to 1m and channel width ranged from 20-50 m. Average sediment size varied greatly between each location. Some sites had a maximum rock size of cobbles <5 cm (Fig. 6) and other locations had large boulders up to 3-5 m (Fig. 5 and 6). In areas with majority cobbles and boulders, we searched for pockets of sand and finer sediment to collect sediment. Detailed descriptions of each site are in Appendix A.

Lab Analysis

The geochemical analysis leaches acid-extractable grain coatings as a proxy for meteoric ^{10}Be. We adopted our leaching methods from Greene (2016). We analyzed sediment in two different grain sizes, fine-grained (<63 μm) and coarse-grained (>250-850 μm), from each of the 20 sampled watersheds. We dried a full watch glass of each sediment sample in the oven, powdered the coarse-grained sediment in a shatter box and placed ~5g of sample of both sediment sizes into a vile. To leach the 40 samples, we added 2 mL of 6M HCl to 0.5 g of sample in a centrifuge tube and placed the sample in a heated sonic bath for 24 hours. Leaching grains in 6M HCl effectively removes grain coatings without affecting the underlying grain matrix (Greene 2016). We centrifuged each sample and separated the leachate from the sediment. To prepare the leachate for ICP-OES analysis using a 1:370 (sample:acid) ratio, where the acid is a 1% HCl and 1% HNO_3 solution. We prepared the High-Purity Standard QCS-27 to have the

same sample:acid ratio. We sent the samples to the Nano Research Facility (EECE) at Washington University in Saint Louis where they analyzed the concentrations of Al, Fe, Mn, Na, Ca, K, Mg, Si and Ti in an ICP-OES.

Measuring $^{10}Be_m$

We measured $^{10}Be_m$ concentrations of both the fine-grained and coarse-grained sediment of 8 watersheds selected arbitrarily. These watersheds include Picard, Macoucherie, Belfast, Mamelabou, Pagua North, Pagua South, Castle Bruce, and White. Using methods from Stone (1998), the sediment was powdered, ^{9}Be carrier added and beryllium extracted at the University of Vermont. $^{10}Be_m$ concentrations were measured with accelerator mass spectrometry (AMS) at Lawrence Livermore National Laboratory.

Microscopy Analysis

We performed microscopy analysis on two coarse-grained samples, Belfast and Mamelabou, chosen due to a visible difference in weathering between the coarse grain samples. We analyzed both samples under the microscope to understand grain composition and grain coating composition. Furthermore, we analyzed the same samples under the SEM to collect an electron image and elemental maps of the coarse grains.

ArcGIS Analysis

We used GIS to calculate zonal statistics within the 20 watersheds of the following basin average parameters: geology, land use, precipitation, slope, local relief, and landslide frequency. The geology of Dominica is primarily volcanic and can be classified into 6 main categories. Our geology data layer (Roobol and Smith, 2004) classifies the rock types into Andesitic Dacite Lava, Block and Ash Flows, Block and Ash Flow Ignimbrites, Ignimbrites, Sedimentary and Volcanics. We accessed our land use map from the Caribbean Handbook on Risk Information

management (CHARIM) database (Dominica, 2016). The land cover map was generated by image classification of satellite images acquired between 1996 and 1999 as part of the Caribbean Land Cover project. Originally, the land use map consisted of 15 classifications and we simplified the categories into five main classifications: Forest, Urban, Agriculture, Grasslands, and Other. To calculate precipitation we digitized the mean annual precipitation map from Lang (1967). We downloaded global DEM data (NASA/METI/AIST/Japan Spacesystems and U.S./Japan ASTER Science Team, 2009) and used the layer to calculate slope and local relief using the Slope and Focal Statistics (circle neighborhood with a 30 cell radius) tool, respectively. To quantify landslide density, we adopted the landslide layer from van Westen (2016)—which mapped landslides pre- and post-Tropical Storm Erika in 2015 using satellite imagery. We quantified the percentage of landslide area per watershed area of pre- and post-TS Erika landslides.

Results

Microscopic Investigations

The two coarse samples, Belfast and Mamelabou, microscopically revealed complex grain mineralogy and low and high total concentrations of acid leachable elements. The Belfast sample (Fig. 7) is evident of the complex grains collected in the detrital sediment. Both single mineral grains and volcanoclastic grains are present in a single sample. The SEM analysis (Fig. 8) reveals grains with high levels of Si, O and Al consistently present throughout the grains, indicating the grains are a type of feldspar. The spectral pattern of consistent Fe indicates Fe is also present within the grain composition. Conversely, isolated bright patches of Fe and Ca reveal grain coatings adhering to the grain concavities (Fig. 8). Little to no evidence of Na and Mn exists within the SEM-EDS analysis. The optical scope found that the concavities within the

feldspars contain the weathered grain coatings. The Mamelabou sample (Fig. 9) contains highly weathered grains with overall distributed concentrations of Si, Al, and O, indicating the grain mineralogy is dominated by feldspars. The Mamelabou grains appear more weathered than the Belfast sample based on the optical analysis presenting relatively higher concentrations of Fe and Ca. The SEM analysis additionally reveals scattered concentrations of Mn, Mg and K in small bright patches on the grain. Therefore, grain coatings may consist of Fe, Ca, Mn, Mg and K.

Grain Coating Concentrations

The ICP-OES analysis revealed the elemental concentrations of HCl-extractable coatings consists of six elements; the standard curves for Al (396.153), Fe (259.939), Mn (260.568), Na (589.592), Mg (280.271), Si (288.158), Ti (336.121) showed statistically significant correlations between counts per second (cps) and standard concentrations. We use these wavelengths to calculate the elemental concentrations of both the coarse- and fine-grained samples, (Table 1) with the exception of calcium for which no useable data was returned.

In the fine-grained sediment, a strong positive correlation exists between Al vs Fe (R^2 is 0.7445), Al vs Mn (R^2 is 0.546), and Fe vs Mn (R^2 is 0.6397) (Fig. 10a). The range of Al, Fe, and Mn concentrations are 2619-6033 ppm, 3457-7678 ppm, and 66 -212ppm, respectively. The Espagnole watershed is an outlier, with negative values for Fe and Mn, and a low value of 101.794 ppm for Al. The correlation between Al, Fe, and Mn shows a relationship concerning the relative concentration of these elements per sample. The accumulation of any one of these elements within a sample is governed by a direct relationship with the other two elements. Conversely, there exists no relationship between Na, K and Ti demonstrating no correlation in relative concentration. Based on prior assumptions (Greene, 2016), the total concentration of grain coatings will be processed as the summation of Al, Fe and Mn concentrations.

The coarse-grained samples show no significant correlation between Al vs Fe (R^2 is 0.0556). A strong correlation exists between Al vs Mn (R^2 is 0.4097) and Fe vs Mn (R^2 is 0.6807) (Fig. 10b). The range of Al, Fe, and Mn concentrations are 1346-5768 ppm, 2229-1380 ppm, and 17-132 ppm, respectively. We calculate the total concentration of grain coatings by the summation of Al, Fe, and Mn to remain consistent with the methods of the fine-sample grain coatings.

Meteoric 10Be

Meteoric ^{10}Be concentrations from 8 watersheds—determined from both coarse- and fine-grained samples—correlate to only some elemental concentrations of Al, Fe, Mn, Na, Mg and Ti. Meteoric ^{10}Be correlates positively with elemental concentrations of Al, Fe and Mn, but inversely with Na (Fig. 11). Meteoric ^{10}Be concentration is unrelated to Mg and Ti concentration. The positive correlations between $^{10}Be_m$ and only Al, Fe, and Mn reinforce the assumption to calculate the total concentration of grain coatings as the summation of Al, Fe and Mn.

Landslides

Landslide density using pre-Erika landslides and post-Erika landslides (Fig. 12) (van Westen, 2016) decreases within the northern and northeastern watersheds on Dominica with a range of 0.5-1.3% (Fig. 13). The lowest density is the Mamelabou watershed, with a density of 0.0459%. Landslide density increases in southern watersheds with a range of 1.3-3.2% Rosalie has the highest density of 3.2% of the watersheds. The northwestern watersheds have an intermediate landslide density of 1.1-2.4%.

Landslide density is inversely and strongly related to the total fine-sample grain coating concentrations with an R^2 value of 0.3054 (Fig. 14a). The Rosalie watershed is an outlier with a

landslide density of 3.31% and a grain coating concentration of 10188.8 ppm. Other watersheds with a similar grain coating concentration contain a landslide density of about 1.3%. The coarse-sample grain coating concentrations show an inverse but weak relationship with landslide density (Fig. 14b). Alternatively, the relationship between $^{10}Be_m$ concentrations and landslide density (Fig. 14c), show a strong inverse relationship similar to the fine-sample grain coating concentrations and landslide density.

Watershed Characteristics

Watershed characterization provides a broader view of controls on weathering and erosion within each watershed (Fig. 15). The relationship between mean annual rainfall and landslide density (Fig. 16) shows no significant relationship. Mean annual rainfall varies little between watersheds; the general trend shows consistent total rainfall with a range of 3.4-6.1 m/yr and total precipitation increases slightly in the southern watersheds. Alternatively, precipitation increases with elevation within each watershed (Fig. 15).

The northeast watersheds have the lowest average slope (15-18^o), the southern watersheds are the steepest (20-27^o), and the northwestern watersheds are intermediate (18-20^o). Slope is weakly correlated to landslide density (Fig. 17). The Mamellabou, Toulaman, Melville watersheds have the lowest slope (15.1-16.5^o) values and landslide densities (0-0.5%). The steepest watersheds, Rosalie, White, Geneva (23.7^o ,27.1^o and 26.23^o, respectively) do not perfectly correlate with landslide density. Rosalie has the highest landslide density (3.2%) but White (2.0%) and Geneva (1.1%) have an intermediate landslide density. Alternatively, the Layou has the second highest landslide density (2.4%), but has a relatively shallow slope (16.3%). Local relief shows similar trends to slope (Fig. 18), showing a positive relationship between local relief and landslide density The northeast watersheds have lower local reliefs

(269-407 ft.), the southern watersheds have the highest local reliefs (512-639 ft.), and the western watersheds have mid relief values (406-471 ft.).

The main variation of volcanic flows between watersheds is the abundance of ignimbrites and block and ash flows (Fig. 19). In general, areas abundant in block and ash flow (>70%) have relatively lower landslide density. The relative amount of ignimbrites increase in the Lamothe (34%), Rosalie (46%), Roseau (36%), Machoucherie (49%) and Espagnole (50%) watershed but only the Rosalie, Roseau, and Macoucherie watersheds have high landslide densities (3.2%, 2.2% and 2.1%, respectively). The Espagnole watershed does not follow this trend, with a relatively low landslide density of 0.5% and the Lamothe watershed has an intermediate landslide density (1.3%). Moreover, the Layou watershed has the second highest landslide density (2.4%) but has an intermediate ignimbrite abundance (20.31%). Generally, watersheds with a landslide density less than 1.3% have a total ignimbrite abundance less than 10% and a block and ash flow abundance greater than 70%.

Overall land use and landslide density show a weak correlation (Fig. 20); but forest abundance follows a similar trend with slope and relief. By watershed, agriculture areas range from 12.31-50.33% and forested areas range from 47.63-83.81%. Urban and grassland areas range from 0.12-3.5% and 0.09-2.88%, respectively. The main variation in land use is between forest and agriculture, while urban and grassland areas contribute only marginally to the total land use.

Discussion

Acid-extraction of detrital sediment grain coatings on Dominica provides a valid proxy for $^{10}Be_m$. Specifically, grain coating concentrations leached from fine sediment significantly relate to landslide density and hence erosion mechanisms in the 20 study watersheds. In this

discussion, we address the implications associated with HCl-extractable grain coatings and the relationship with $^{10}Be_{m.}$ Then we utilize our proxy to evaluate general erosional processes within 20 study watersheds and we consider the effects of watershed characteristics on the data set. Finally, we assess our methods to address assumptions and suggest improvements.

Approximating Meteoric ^{10}Be

HCl-extraction predominantly leached Fe and Al, suggesting reactive grain coatings are composed of these minerals. The large concentrations of Fe found in the ICP-OES analysis suggest that the bulk of the grain coatings are composed of amorphous Fe oxy-hydroxides (Singleton et al., 2017; Greene, 2016; Wittmann et al., 2012). The SEM-EDS revealed large concentrations of Fe in isolated patches on the coarse-grained samples, which is inferred to be the sampling material of the HCl-extraction. Additionally, acid-extractable Al is part of the weathering material; the large concentrations of Al suggest some of the grain coatings are composed of Al oxy-hydroxides (Greene, 2016). The grain compositions include volcanoclastics and feldspars (Fig. 7), which are high in Si, O and Al. The HCl method, however, effectively removes grain coatings without dissolving the underlying mineral matrices of the detrital sediment and leaves quartz, feldspars and micas undissolved (Greene, 2016; Singleton et al., 2017). The HCl method primarily leaches crystalline and amorphous oxides/hydroxides (Greene, 2016), therefore the grain coating concentrations are primarily composed of Fe and Al oxide weathering products.

The total concentration of acid-extractable Fe, Al and Mn is a valid proxy for $^{10}Be_m$ in detrital sediment. When meteoric ^{10}Be reaches the surface, the atoms bind tightly to soil and sediment particles because of the reactive nature of $Be(OH)_2$ (Willenbring, 2010). Singleton et al. (2017) found $^{10}Be_m$ is strongly correlated with acid-extractable elements, which in turn is

positively related to the accumulation of reactive phases during pedogenesis. The elements Fe and Al and Mn are site-dependent; Dominica samples vary from the elements selected in Singleton et al. (2017) and Greene (2016). It is evident through a positive relationship between Fe and Al (Fig. 10) that these elements accumulate directly within grain coatings during pedogenesis on Dominica. Mn—which has a concentration an order of magnitude lower than Fe and Al—also shows a direct relationship with Fe and Al (Fig. 10); suggesting Mn accumulates similarly within grain coatings. Furthermore, the HCl-extractable elements of Fe, Al, and Mn show a positive correlation with meteoric ^{10}Be (Fig. 11); consistent with Greene (2016), who found acid-extractable Fe, Mn and Al strongly and positively correlate with $^{10}Be_m$ concentrations. Therefore, the total concentration of grain coatings is composed of Fe, Al and Mn, based on the relationship in which each element directly accumulates in grain coatings and directly relates with $^{10}Be_m$.

Alternatively, Na, Mg and Ti are excluded from our measure of the total concentration of grain coatings based on the absence of a direct positive relationship (Fig. 10). Compared to the total concentration of grain coatings; Na is inversely correlated, and Mg and Ti are positively but weakly correlated. Additionally, when compared to $^{10}Be_m$, Na is inversely correlated and Mg and Ti show no correlation. Na may have an inverse relationship with grain coatings and $^{10}Be_m$ due to the leaching of Na through soil, rather than accumulating into grain coatings during pedogenesis (Birkeland, 1999). Mg and Ti may have a weak/lack of correlation due to the resistant weathering nature of Mg and Ti oxides (Birkeland, 1999). These elements do not behave in the same manner as Fe, Al and Mn during pedogenesis, and therefore do not follow of the direct relationship between grain coatings and $^{10}Be_m$.

Characterizing Erosional Processes

Based on the strong positive relationship between elemental concentration of grain coatings and $^{10}Be_m$, grain coatings will behave similarly to $^{10}Be_m$ as a sediment tracer (Fig. 11). When compared to landslide density, both fine-sample grain coatings and $^{10}Be_m$ show a strong inverse relationship (Fig 14a, 14c), suggesting both tracers reveal similar erosional processes. Alternatively, coarse-sample grain coatings compared with landslide density show an inverse but weak relationship (Fig. 14b); this relationship may be a result of one of the major assumptions in sediment tracing. We assumed that grain coating concentrations are associated only with upland erosion processes and not transport processes. Coarse-grained material moves down a river system by saltation, rather than as suspended load like the fine-grained sediment (Thompson and Turk, 1991). The abrasion of coarse-grained material may decrease the total concentration of grain coatings, depending on transport distance. The use of coarse-grained sediment for sediment tracing has complications brought on by the effects of transport processes on the concentration of grain coatings, and may misrepresent the total concentration of grain coatings. Further work would account for transport distance by collecting sediment with a range of transport distances within a single watershed. Sourcing sediment closer to the erosional processes would better account for transport distance and be more representative of the hillslope erosion processes. In this study, the fine-sample grain coatings are a more viable sediment tracer than the coarse-sample grain coatings when assessing basin-scale erosional processes.

The erosional processes on Dominica can be interpreted using fine-sample grain coatings as a sediment tracer proxy for $^{10}Be_m$. The northeastern watersheds with high grain coating concentrations have mostly shallow erosional processes (Reusser and Bierman, 2010). Shallow erosion allows time for accumulation of $^{10}Be_m$ grain coating concentrations (Reusser and

Bierman, 2010). Low landslide densities in the northeastern watersheds and high grain coating concentrations show that deeply sourced sediment is not a main contributor to outlet sediment. The southern watersheds contain lower concentration of grain coatings, suggesting the erosional processes are sourcing rapidly eroded material or deep material. Rapidly eroding and deep-sourced sediment fail to accumulate $^{10}Be_m$ and correspondingly, grain coating concentrations (Reusser and Bierman, 2010). The correlation of low grain coating concentration with high landslide density in these watersheds supports the idea that landslides are significant contributors to the outlet sediment. Therefore, the outlet sediment is characteristic of the erosional processes in the corresponding watersheds.

Evaluating Watershed Characteristics

Differences of rainfall, slope, local relief, geology and land use between the 20 watersheds account for the diverse erosional processes on Dominica. Even though precipitation is the main mechanism for inducing landslides (De Graff et al., 1989), the little variability of mean annual rainfall fails to explain changes in landslide density between watersheds. However, landslides instead can be initiated by single heavy precipitation events. Nugent and Rios-Berrios (2017) mapped radar-derived precipitation values for Tropical Storm Erika over a 24 hour period on August 27, 2015 (Fig. 21). Mapped isohyets from this storm correlate weakly with TS Erika induced landslides (van Westen, 2016). Areas with the highest rainfall follow the highest topography, located centrally in the northern and southern areas of Dominica. The northern watersheds that intersect with areas of high rainfall only partially correlate with landslide density. The Hampstead, Batali, and Macoucherie Watersheds intersect with high isohyets and have a high Erika induced landslide density. Conversely the Melville watershed, which intersects most of the area with high isohyets, has a low Erika induced landslide density. In the southern

area, the White watershed intersects the isohyets with the highest rainfall and has a high Erika induced landslide density. Alternatively the Roseau and Geneva watersheds partially intersect with the high isohyets but have a low landslide density. Thus, landsliding events may be induced by single storm events, rather than mean annual rainfall, but clearly other factors must still affect landslide density.

Mean slope and local relief strongly correlate with landslide density and both factors are important drivers for erosional processes on Dominica. While areas with the steepest slopes have the highest landslide density, Andereck (2007) found that areas with slopes of 16 to 24 degrees have the highest landslide density. Andereck (2007) speculates that areas with this range of slopes are shallow enough for soil development, but are steep enough to have favorable conditions for initiating landslides. Therefore, our data may be too generalized to fully understand the relationship between slope and landslides, but we can note the strong positive correlation between landslides and slope.

Andereck (2007) found an inverse relationship between active agriculture and landslides, suggesting the presence of agriculture decreases the probability of landslides. This finding corresponds with our data, where areas with low landslide density have the highest agriculture activity. However, we speculate this relationship because active agriculture includes banana and dasheen cultivation, which have poor root systems and exposed soil (Andereck, 2007). Active agriculture areas which include this type of cultivation would thus increase landslide density (De Graff, 1990). Therefore, landslides behave differently with variations in agriculture. Moreover, heavily forested watersheds had a higher landslide density, and Andereck (2007) found a similar relationship. We again speculate because evergreen forest is found in areas with higher elevation and steeper topography (Andereck, 2007) which may dominate the relationship between land

cover and landsliding. Finally, the weak correlation with landslide density and geology suggests that variability in rock type plays only a minor role in erosional processes. The high percentages of ignimbrites in the Rosalie, Roseau and Macoucherie watersheds suggest that these flows are less resistant to weathering and may provide a bedrock condition that is conducive to landslides. However, further information is needed on the relative strength of the different geologic units.

It is clear that grain coatings can be related to erosion by landslides, but many other factors contribute variation in our bivariate experiment and must be explored further. We looked at common variables that could affect landslide density. However, further work should investigate variables which would affect grain coating concentration. Hydrothermal areas are dispersed throughout Dominica and may further complicate the relationship between grain coating concentration and erosion. The effects of hydrothermal alteration are similar to the products of weathering (Kerr, 1955); variable pedogenesis may affect the production of grain coatings. Furthermore, variations in rock age may result in differences in weathering, and thus affect both grain coatings and erosion. Mobility of elements within the surrounding soil decreases with rock age due to the lesser amount of soluble parent rock (Gislason et al., 1996).

Conclusion

This work continues the nascent efforts to characterize erosional processes on Dominica outside of landslides. This study shows that fine-sample grain coating concentrations from detrital sediments works as a proxy for $^{10}Be_m$ in order to interpret upstream erosional processes. In Dominica, grain coatings primarily consist of Al, Fe and Mn. Total concentration of these elements negatively correlated with mapped landslides. The correlation between coatings from fined-grained samples and landslides, suggests that landslides are a significant erosional process

within Dominican watersheds. Scatter in this relationship likely falls to environmental factors such as rainfall distribution of a single event, slope, land use and geology.

Acknowledgements

Thank you to the Keck Geology Consortium and the Kozak, Spencer, McGuire, Schwab Award for making this research project possible. Special thank you to my Washington and Lee advisors, David Harbor and Margaret Anne Hinkle, and my Keck Project advisor, Amanda Schmidt. Additional thanks to Emily Falls and Sarah Wilson at Washington and Lee University, and Holli Frey, the Head Keck Project advisor. Finally, thank you to the Team Geomorph members, Haley Talbot-Wendlandt, Cole Jimerson and Marcus Hill.

References

Andereck, Z.D., 2007, Mapping Vulnerability of Infrastructure to Destruction by Slope Failures on the Island of Dominica, WI: A Case Study of Grand Fond, Petite Soufriere, and Mourne Jaune [Master of Arts]: Miami University, 72 p.

Birkeland, P.W., 1984, Soils and Geomorphology: Oxford University Press, 372 p.

Birkeland, P.W., 1999, Soils and Geomorphology: Oxford University Press, 452 p.

De Graff, J., 1987, Landslide hazard on Dominica, West Indies: Final report: The Commonwealth of Dominica and the Organization of American States.

De Graff, J., 1990, Post-1987 Landslides on Dominica, West Indies: An Assessment of Landslide-Hazard map Reliablity and Initial Evaluation of Vegetation Effect on Slope Stability: The Commonwealth of Dominica and the Organization of American States.

De Graff, J., Brice, R., W. Jibson, R., Mora Castro, S., and Rogers, C., 1989, Landslides: their extent and economic significance in the Caribbean, *in* p. 51–80.

Dominica, 2016, Dominica Land cover (2000 updated): Cqaribbean Handbook on Risk Infromation Management (CHARIM).

Frey, H.M., 2016, Dominica: The Sleeping Giant in the Caribbean: F&M Scientist, v. Winter 2016, p. 3–34.

Gislason, S.R., Arnorsson, S., and Armannsson, H., 1996, Chemical weathering of basalt in Southwest Iceland; effects of runoff, age of rocks and vegetative/glacial cover: American Journal of Science, v. 296, p. 837–907, doi: 10.2475/ajs.296.8.837.

Graly, J.A., Bierman, P.R., Reusser, L.J., and Pavich, M.J., 2010, Meteoric 10Be in soil profiles – A global meta-analysis: Geochimica et Cosmochimica Acta, v. 74, p. 6814–6829, doi: 10.1016/j.gca.2010.08.036.

Greene, E.S., 2016, Comparing 10Be, in situ 10Be, and native 9Be across a diverse set of watersheds [Master of Science Thesis]: University of Vermont, 110 p.

Kerr, P.F., 1955, Hydrothermal Alteration and Weathering, *in* Poldervaart, A. ed., Crust of the Earth: A Symposium, Geological Society of America, https://doi.org/10.1130/SPE62-p525 (accessed April 2018).

Lang, D.M., 1967, Soil and land-use surveys No. 21. Dominica.: Soil and land-use surveys No. 21. Dominica., https://www.cabdirect.org/cabdirect/abstract/19721905097 (accessed April 2018).

Lindsay, J.M., Stasiuk, M.V., and Shepherd, J.B., 2003, Geological history and potential hazards of the late-Pleistocene to Recent Plat Pays volcanic complex, Dominica, Lesser Antilles: Bulletin of Volcanology, v. 65, p. 201–220, doi: 10.1007/s00445-002-0253-y.

NASA/METI/AIST/Japan Spacesystems, and U.S./Japan ASTER Science Team, 2009, ASTER Global Digital Elevation Model [Data set]: NASA EOSDIS Land Processes DAAC, https://doi.org/10.5067/ASTER/ASTGTM.002.

Nugent, A.D., and Rios-Berrios, R., 2017, Factors Leading to Extreme Precipitation on Dominica from Tropical Storm Erika (2015): Monthly Weather Review, v. 146, p. 525–541, doi: 10.1175/MWR-D-17-0242.1.

Portenga, E.W., and Bierman, P.R., 2011, Understanding Earth's eroding surface with 10Be: GSA Today, v. 21, p. 4–10, doi: 10.1130/G111A.1.

Reusser, L.J., and Bierman, P.R., 2010, Using meteoric 10Be to track fluvial sand through the Waipaoa River basin, New Zealand: Geology, v. 38, p. 47–50, doi: 10.1130/G30395.1.

Reusser, L., Graly, J., Bierman, P., and Rood, D., 2010, Calibrating a long-term meteoric 10Be accumulation rate in soil: Geophysical Research Letters, v. 37, p. L19403, doi: 10.1029/2010GL044751.

Roobol, M.J., and Smith, A.L., 2004, Geologic Map of Dominica, West Indies:, http://www.charim-geonode.net/layers/geonode:geology_dominica.

Rouse, W.C., Reading, A.J., and Walsh, R.P.D., 1986, Volcanic soil properties in Dominica, West Indies: Engineering Geology, v. 23, p. 1–28, doi: 10.1016/0013-7952(86)90014-1.

Singleton, A.A., Schmidt, A.H., Bierman, P.R., Rood, D.H., Neilson, T.B., Greene, E.S., Bower, J.A., and Perdrial, N., 2017, Effects of grain size, mineralogy, and acid-extractable grain coatings on the distribution of the fallout radionuclides 7Be, 10Be, 137Cs, and 210Pb in river sediment: Geochimica et Cosmochimica Acta, v. 197, p. 71–86, doi: 10.1016/j.gca.2016.10.007.

Sosa Gonzalez, V., Schmidt, A.H., Bierman, P.R., and Rood, D.H., 2017, Spatial and temporal replicability of meteoric and in situ10Be concentrations in fluvial sediment: Earth Surface Processes and Landforms, v. 42, p. 2570–2584, doi: 10.1002/esp.4205.

Stone, J., 1998, A rapid fusion method for separation of beryllium-10 from soils and silicates: Geochimica et Cosmochimica Acta, v. 62, p. 555–561, doi: 10.1016/S0016-7037(97)00340-2.

Thompson, G.R., and Turk, J., 1991, Modern physical geology: Saunders College Publishing, 664 p.

Wallbrink, P.J., and Murray, A.S., 1993, Use of fallout radionuclides as indicators of erosion processes: Hydrological Processes, v. 7, p. 297–304, doi: 10.1002/hyp.3360070307.

van Westen, C.J., 2016, National Scale Landslide Susceptibility Assessment for Dominica:, doi: 10.13140/RG.2.1.4313.2400.

van Westen, C., Zhang, J., and Sijmons, K., 2018, Tropical Cyclone Maria. Inventory of landslides and flooded areas: UNITAR, https://unitar.org/unosat/node/44/2762 (accessed March 2018).

Willenbring, 2010, Meteoric cosmogenic Beryllium-10 adsorbed to river sediment and soil: Applications for Earth-surface dynamics: Earth-Science Reviews, v. 98, p. 105–122, doi: 10.1016/j.earscirev.2009.10.008.

Wittmann, H., Von, B., Bouchez, J., Dannhaus, N., Naumann, R., Christl, M., and Gaillardet, J., 2012, The dependence of meteoric 10Be concentrations on particle size in Amazon River bed sediment and the extraction of reactive 10Be/ 9Be ratios: Chemical Geology, v. 318–319, p. 126–138, doi: 10.1016/j.chemgeo.2012.04.031.

Figures

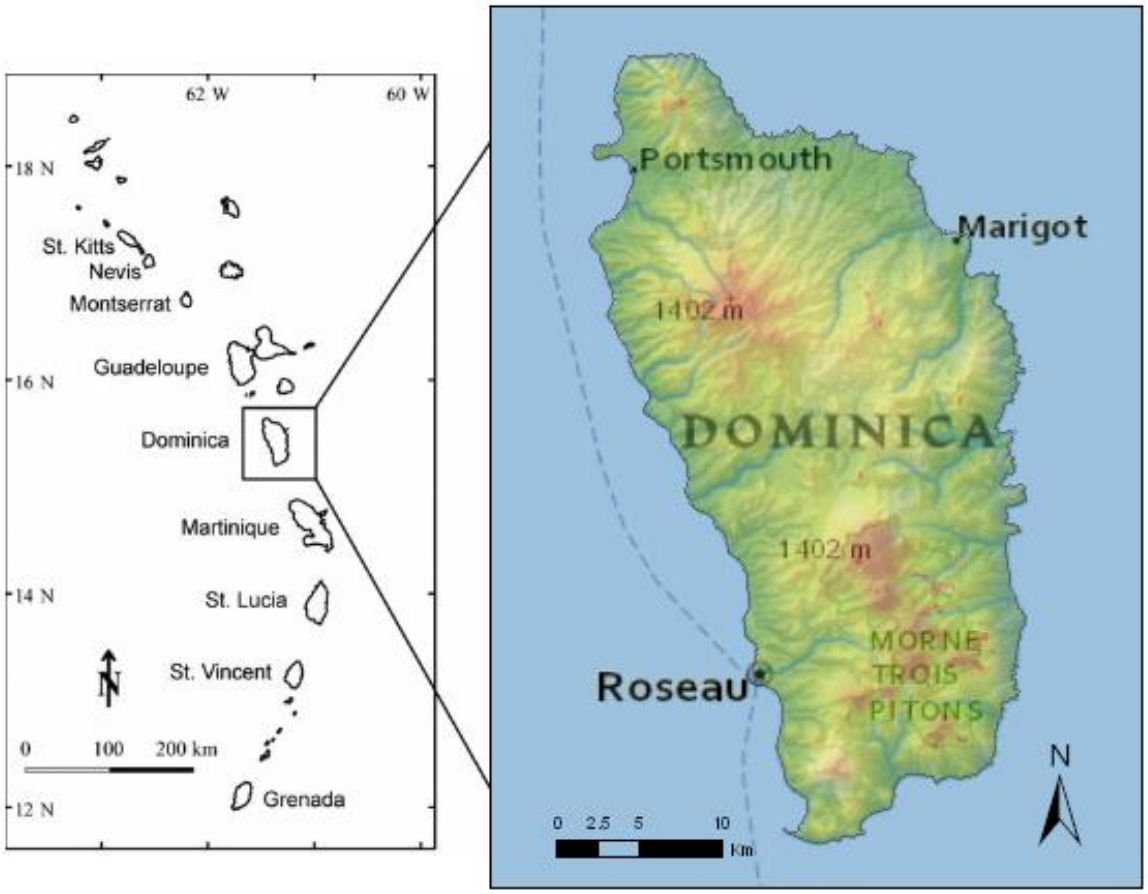

Figure 1. Map of Lesser Antilles Arc (Lindsay et al., 2003) and inset is a DEM (Dominica, 2016) of Dominica.

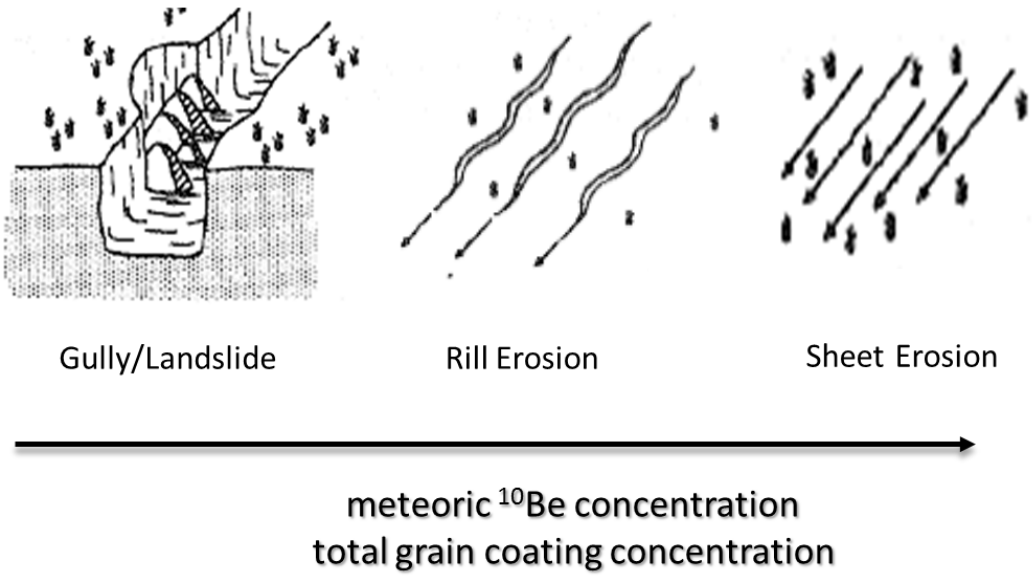

Figure 2. Relative concentration of meteoric ^{10}Be and total grain coatings in types of erosion. Adapted from Wallbrink and Murray (1993).

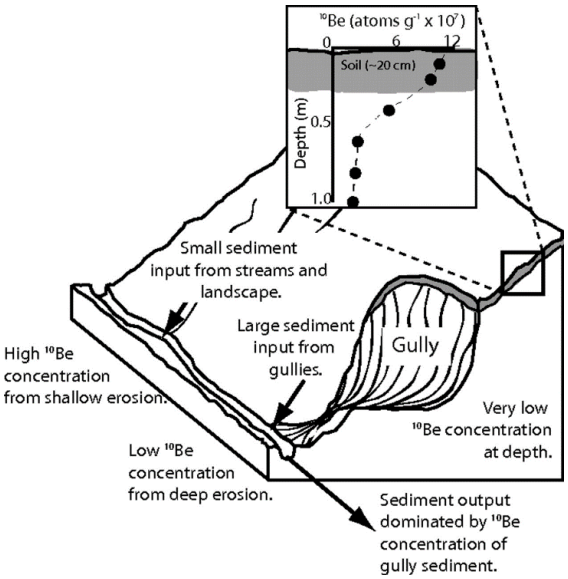

Figure 3. Adopted from Reusser and Bierman (2010), representation of meteoric ^{10}Be activity. Large amounts of deeply sourced sediment contain low ^{10}Be, which will reflect the overall sediment erosion processes in the basin.

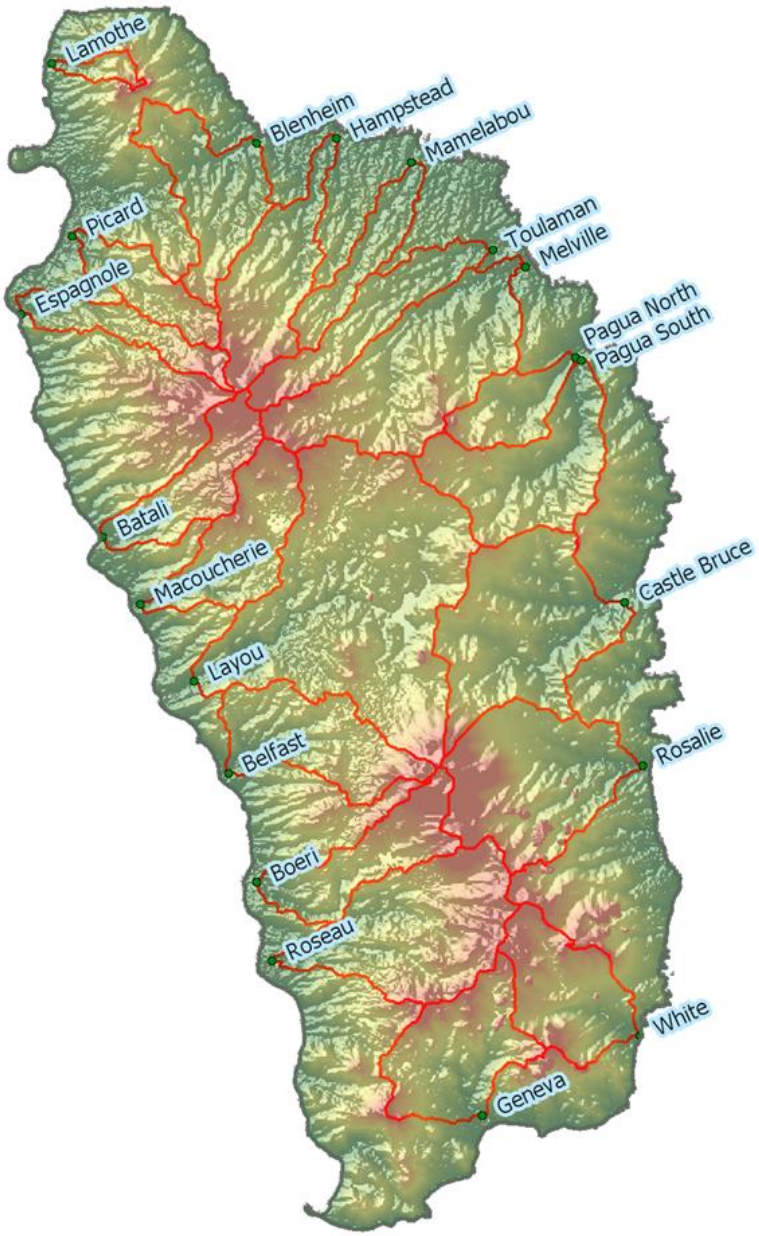

Figure 4. 20 watersheds on Dominica in which we sampled at outlet points (indicated by green points).

Figure 5. White River (DM 17) sample site. Example of urban features near sample sites. Sediment size varies from small cobbles ~5cm to large boulders ~3m. Downstream of the Valley of Desolation.

Figure 6. Blenheim River (DM3) location with highly vegetated banks. Sediment size ranges from fine sediment to cobbles ~10 cm.

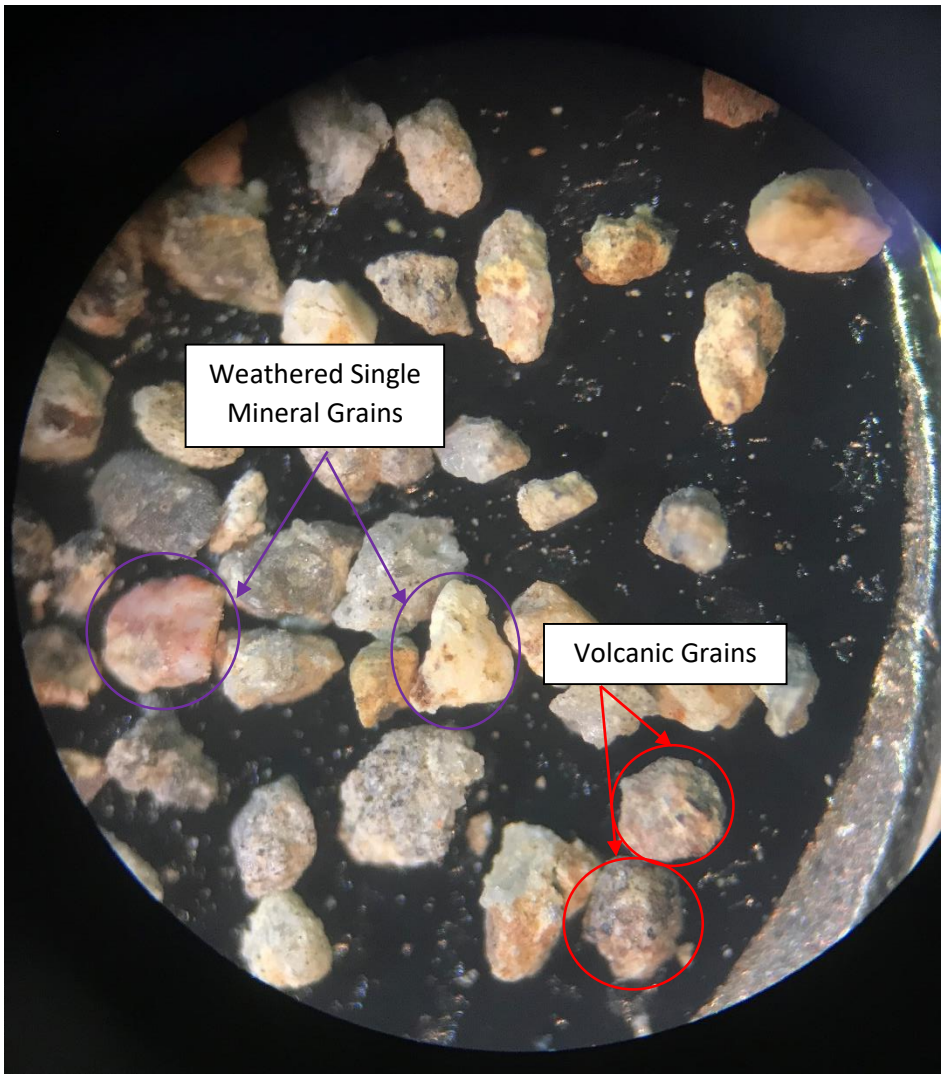

Figure 7. Microscope image of Belfast Coarse Grains. Note the variation in the single mineral grain and multiple mineralogy of the volcanics.

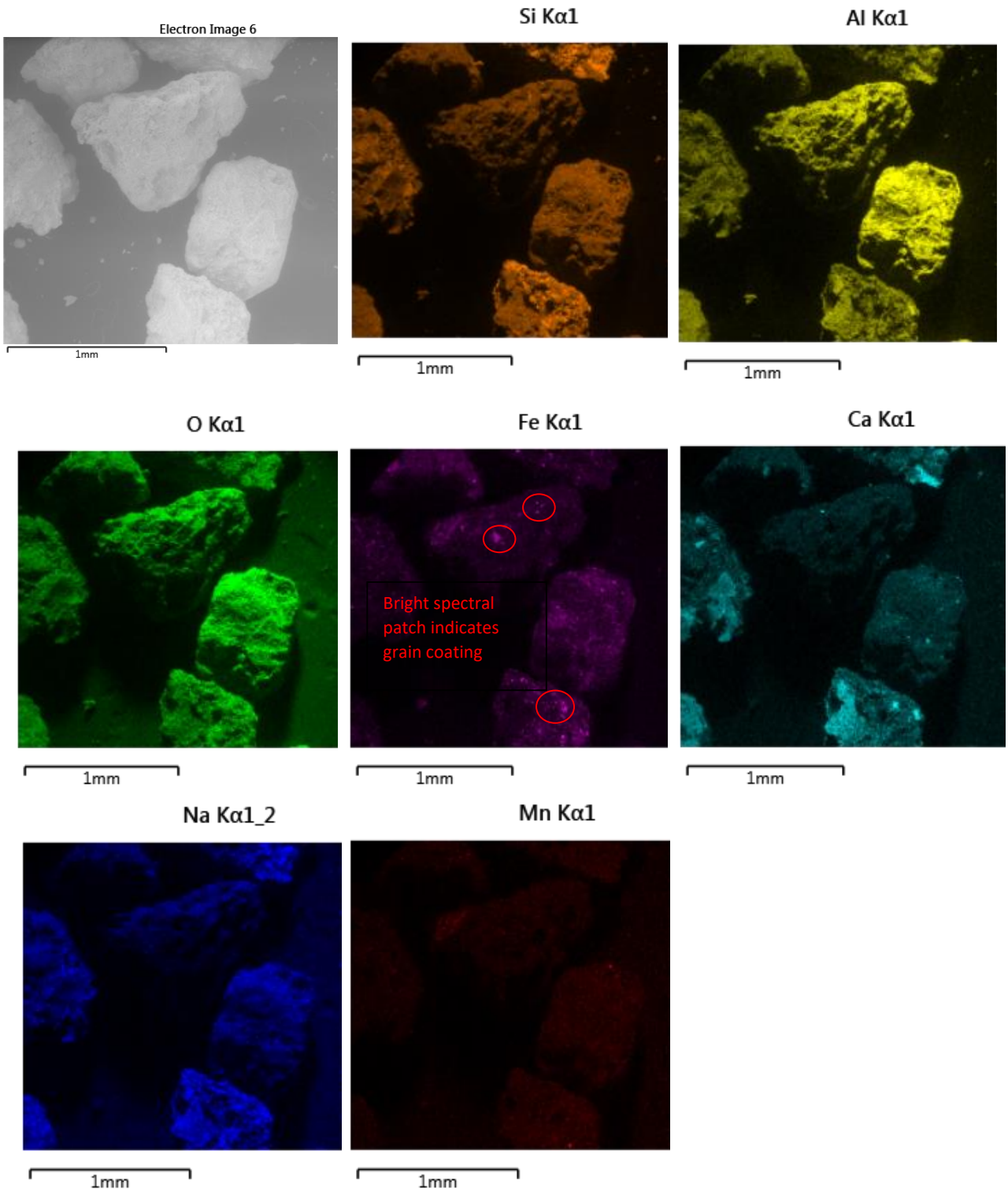

Figure 8. SEM Electron image and elemental maps of coarse-grained samples from the Belfast watershed.

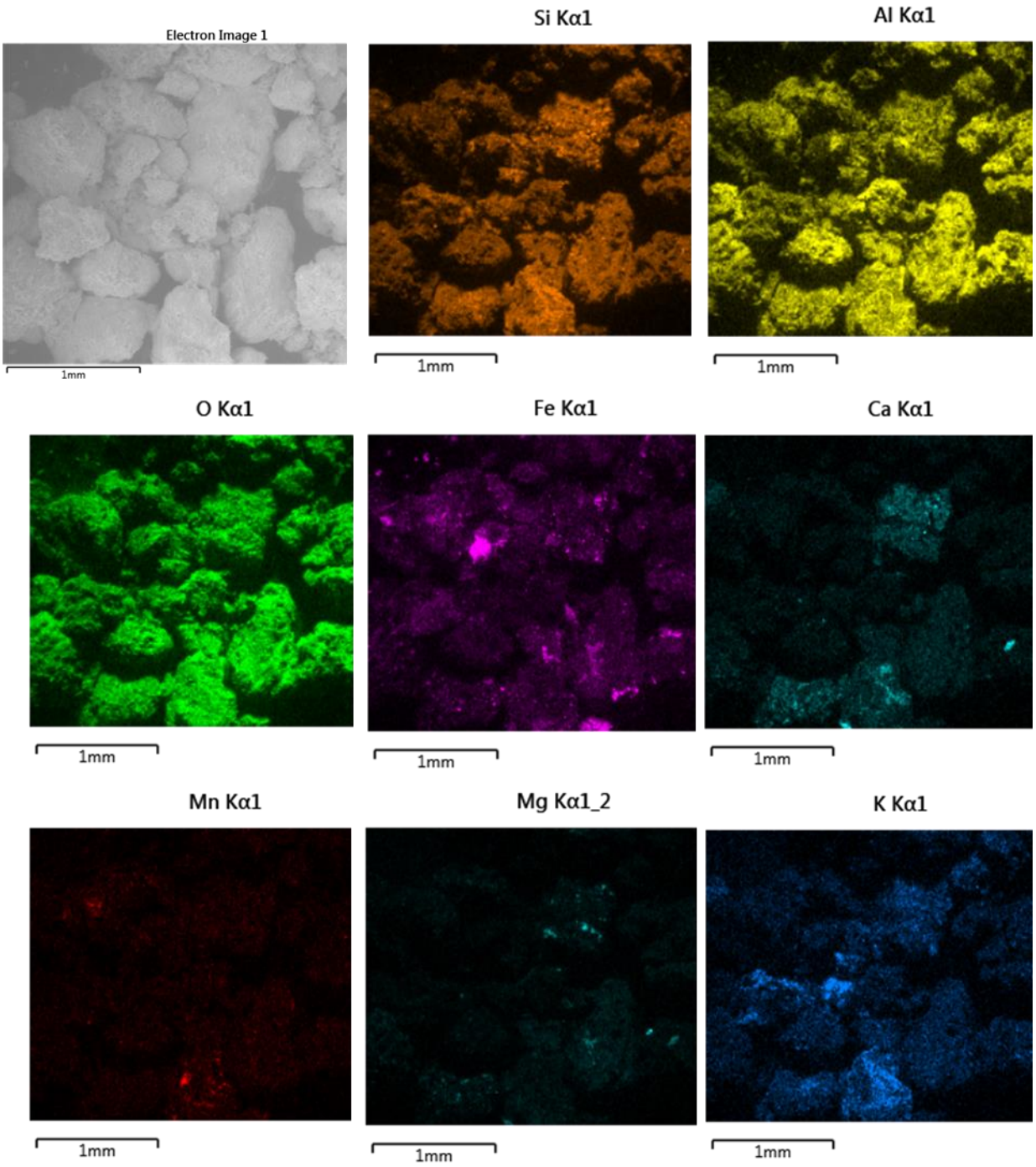

Figure 9. SEM Electron image and elemental maps of coarse-grained samples from the Mamelbou watershed.

Table 1a. Elemental Concentrations in Fine-Grained Samples

FINE							
Name	Al (ppm)	Fe (ppm)	Mn (ppm)	Na (ppm)	Mg (ppm)	Ti (ppm)	Total (ppm)
Lamothe	4554	4603	180	180	193	71	9336
Blenheim	3217	6498	199	111	165	125	9914
Hampstead	4216	5800	117	498	361	221	10132
Mamelabou	5123	6918	156	123	173	161	12196
Toulaman	5145	5592	120	176	362	139	10858
Melville	3327	6116	101	174	327	160	9544
Pagua North	6033	7540	212	129	540	215	13786
Pagua South	5056	7678	169	158	565	144	12904
Castle Bruce	5244	6704	123	207	662	158	12070
Rosalie	4737	5321	131	254	359	135	10189
White	3301	3936	106	254	227	141	7343
Geneva	3529	4474	104	260	400	101	8108
Roseau	2619	3547	67	233	138	88	6233
Boeri	4416	4963	73	417	200	217	9451
Belfast	5638	6571	182	218	275	223	12391
Layou	2784	3762	68	164	198	145	6614
Macoucherie	3349	4531	147	183	407	107	8026
Batali	3811	5311	168	213	369	136	9289
Espagnole	102	-279	-13	54	-101	-6	-191
Picard	3507	5463	104	211	442	89	9075

*Total grain Coating is the sum of Al, Fe, and Mn concentrations

Table 1b. Elemental Concentrations of Coarse-Grained Samples

COARSE							
Name	Al (ppm)	Fe (ppm)	Mn (ppm)	Na (ppm)	Mg (ppm)	Ti (ppm)	Total (ppm)
Lamothe	2519	6749	89	210	208	221	9357
Blenheim	3729	10969	132	213	330	543	14830
Hampstead	2906	6639	65	384	412	396	9610
Mamelabou	4089	12386	122	223	426	910	16598
Toulaman	4527	7662	96	367	610	502	12286
Melville	2823	6147	69	273	487	311	9039
Pagua North	5195	8196	116	231	459	417	13507
Pagua South	5768	8146	119	244	2256	107	14033
Castle Bruce	3097	5892	83	165	567	155	9073
Rosalie	1346	13800	94	191	193	953	15240
White	2119	4005	54	251	268	191	6178
Geneva	2705	3396	38	340	336	153	6139
Roseau	2259	2229	17	350	73	97	4505
Boeri	2260	4633	33	347	105	276	6927
Belfast	3416	5346	61	373	236	335	8823
Layou	2771	5055	50	460	311	316	7876
Macoucherie	2213	6871	70	300	827	436	9155
Batali	2536	6730	68	338	218	435	9334
Espagnole	3078	6243	73	325	428	333	9394
Picard	2964	5501	56	263	354	235	8521

*Total grain coatings is the sum of Al, Fe, and Mn concentrations

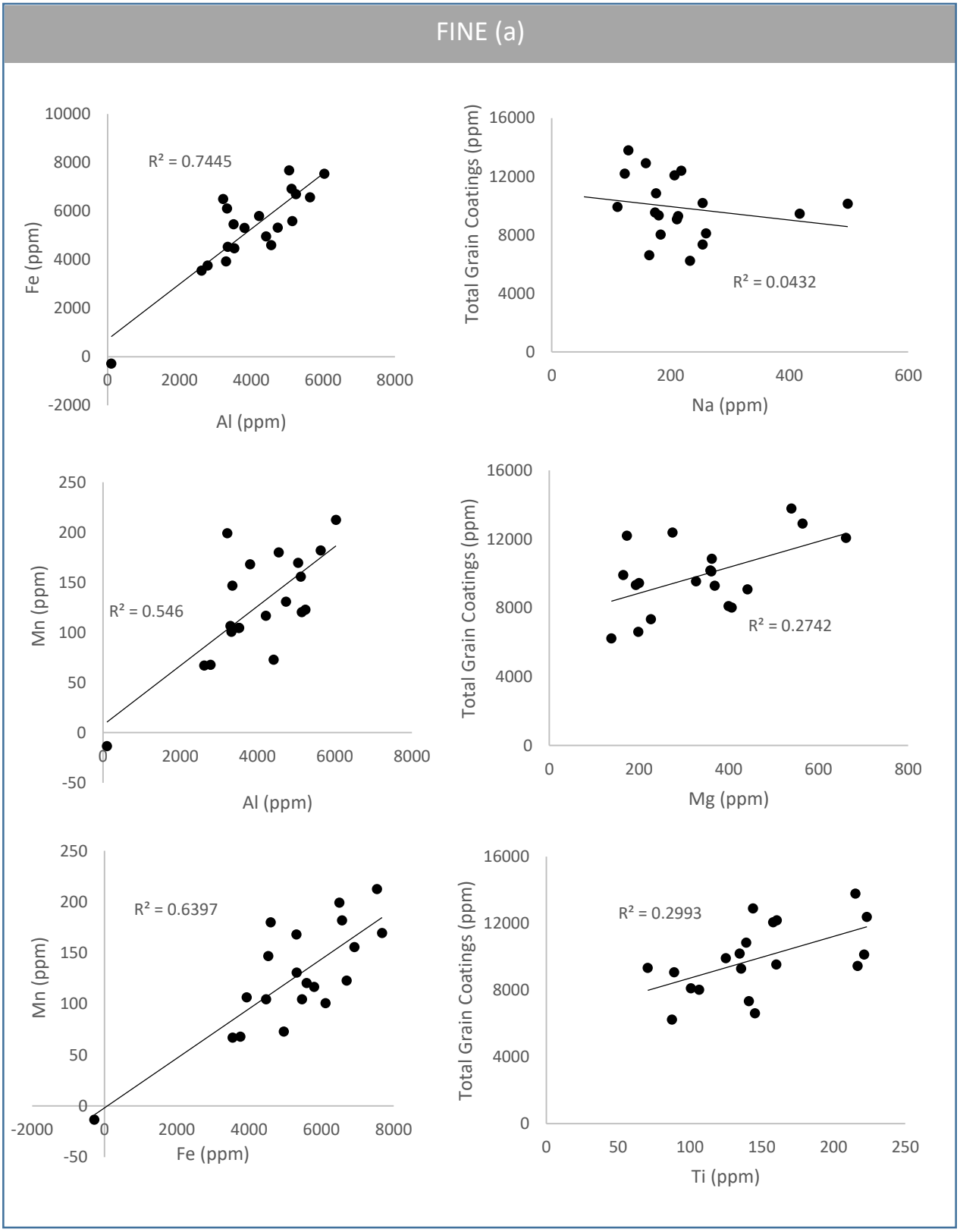

Figure 10a. Concentrations by watershed of Al, Fe and Mn, Na, Mg and Ti. Left) elements compared to each other. Right) Elements compared to Total Coatings.

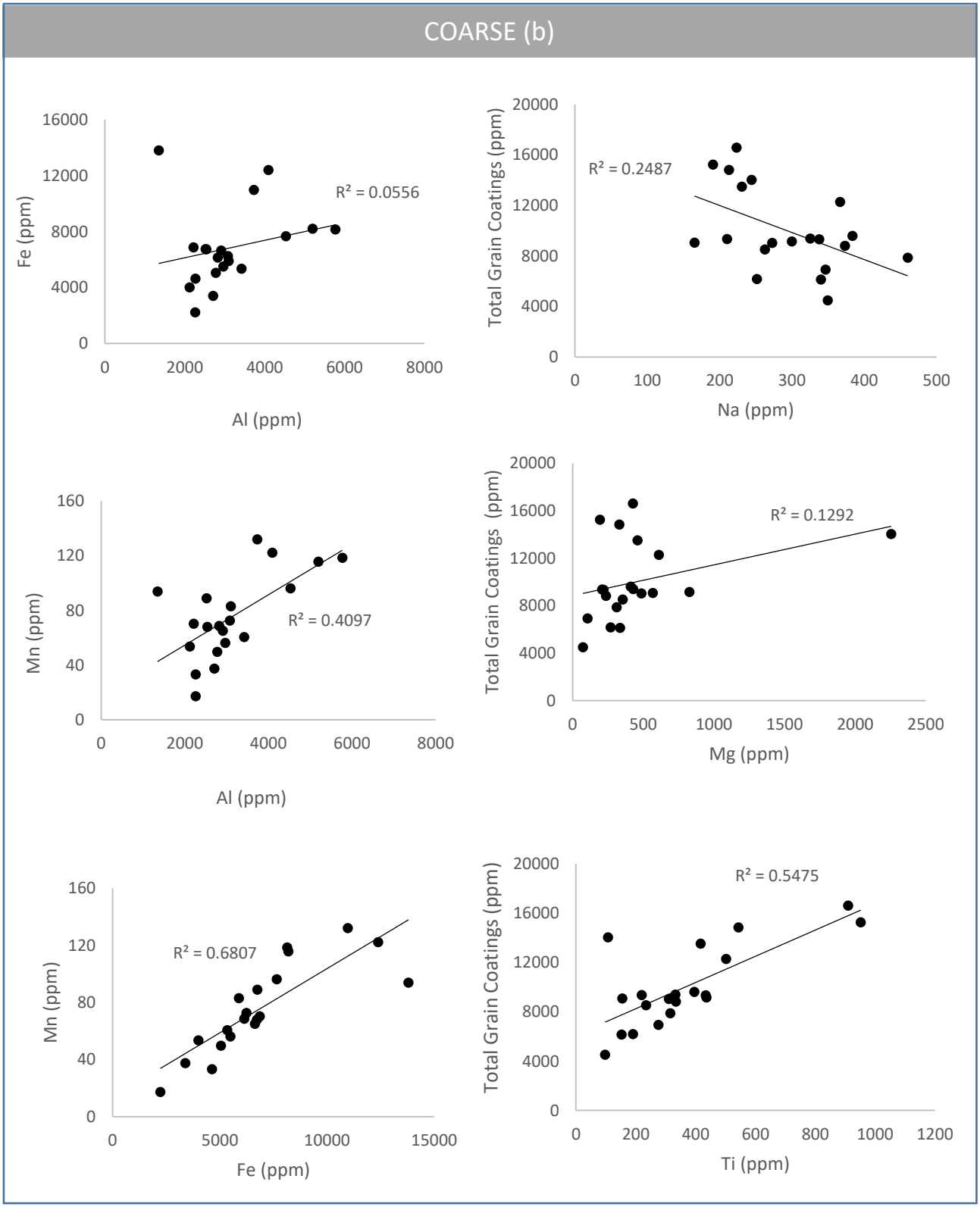

Figure 10b. Concentrations by watershed of Al, Fe and Mn, Na, Mg and Ti. Left) elements compared to each other. Right) Elements compared to Total Coatings.

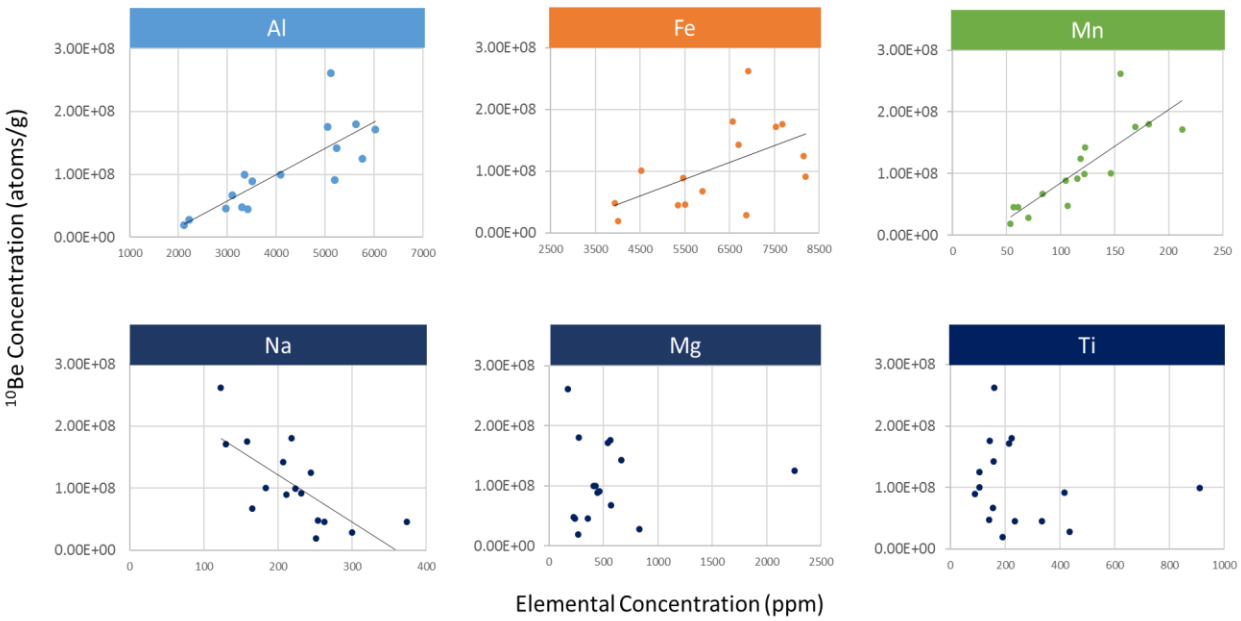

Figure 11. $^{10}Be_m$ vs. combined fine and coarse sample elemental concentrations of HCl-extractable grain coatings.

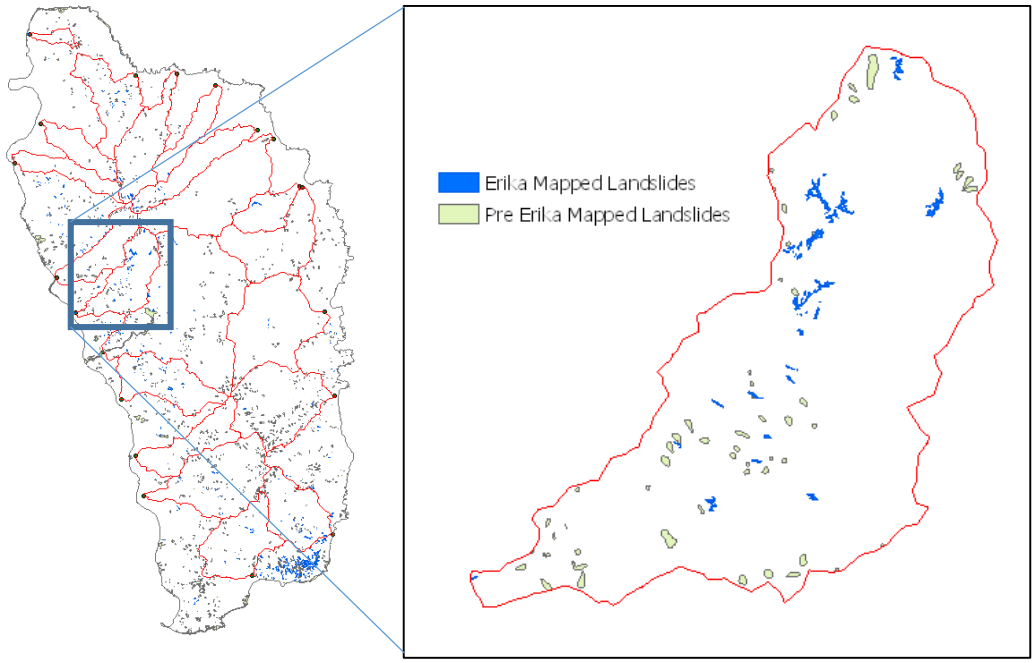

Figure 12. Map of pre-Erika and post-Erika Landslides mapped by van Westen (2016) with an inset for the Macoucherie watershed where landslide density is 2.2%.

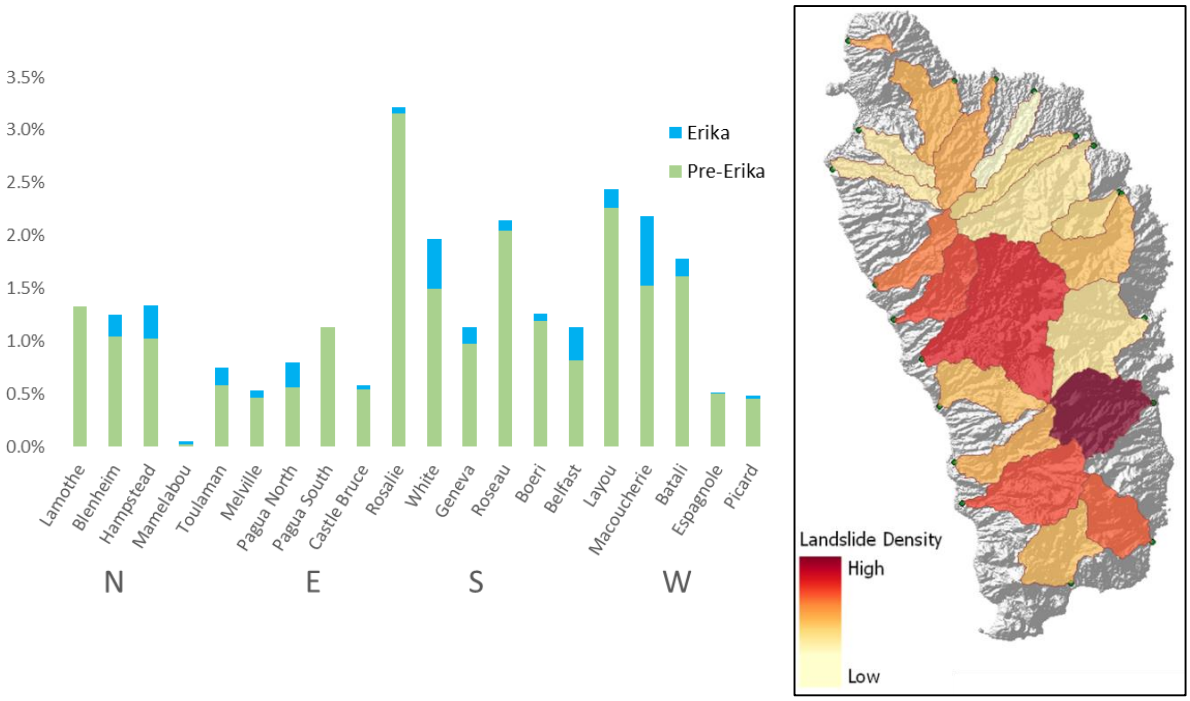

Figure 13. Landslide Density. (Left) Graphical representation (Right) Map representation.

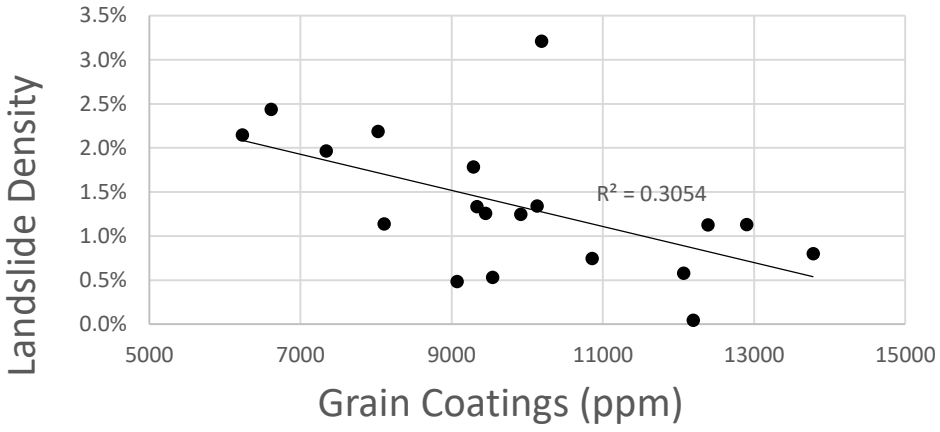

Figure 14a. Fine Grain Coatings vs Landslide Density.

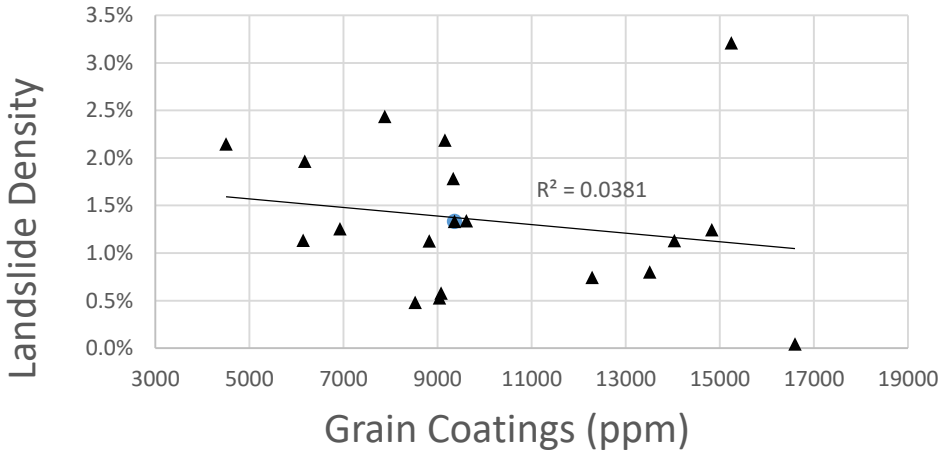

Figure 14b. Total Grain Coatings vs Landslide Density.

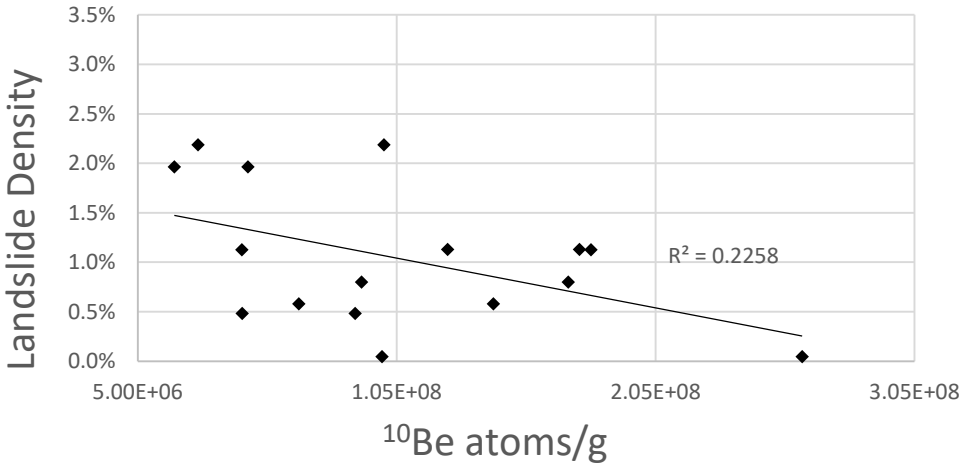

Figure 14c. ^{10}Be atoms/g vs landslide density.

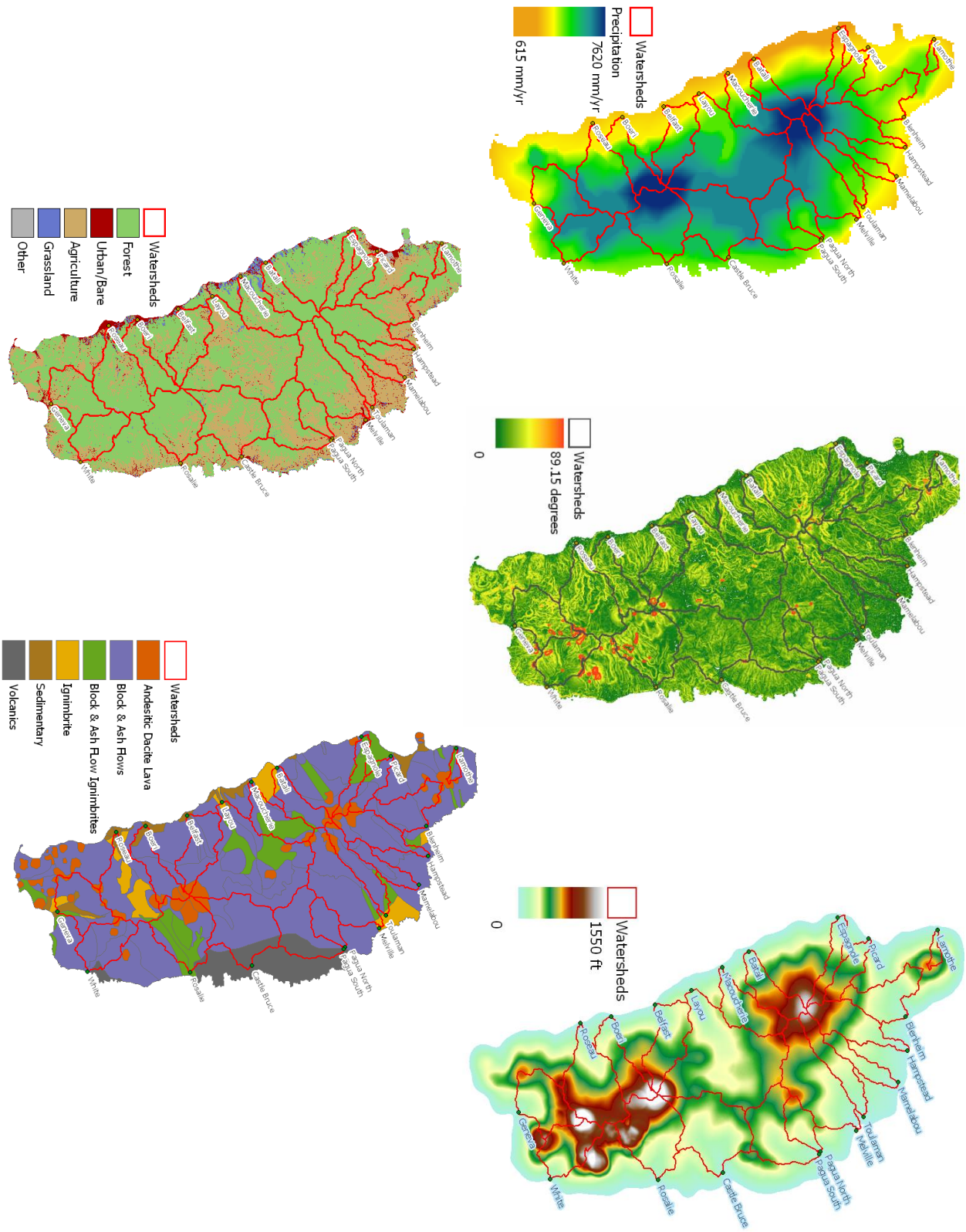

Figure 15. Watershed Characteristics. a) Rainfall b) slope c) local relief d) land use e) geology

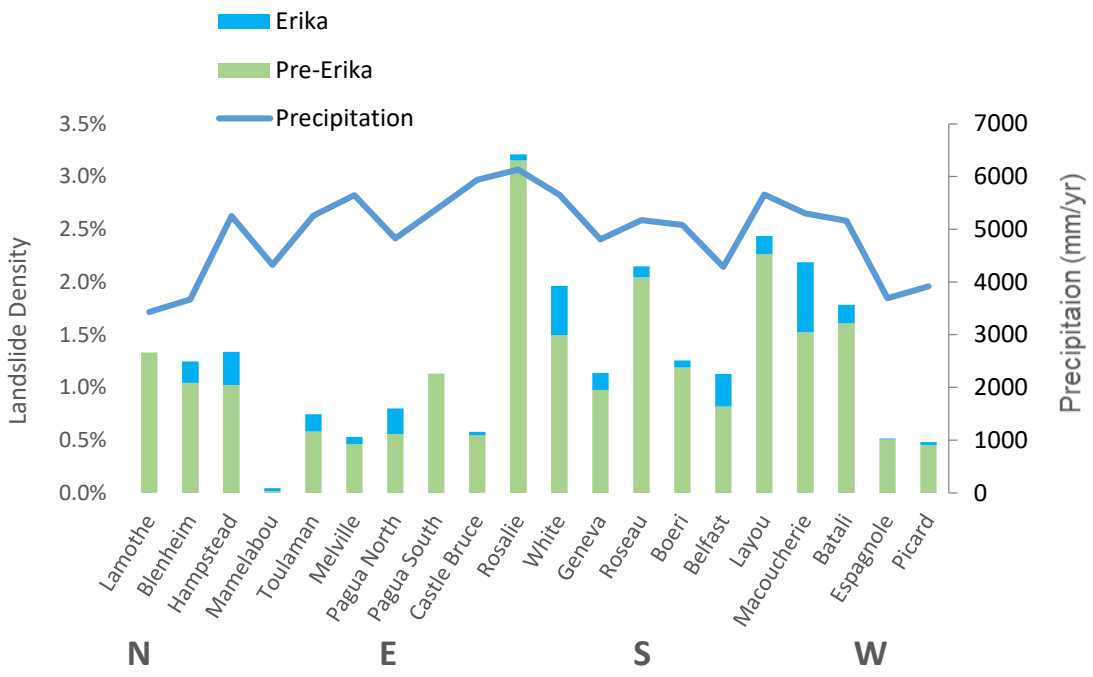

Figure 16. Mean Annual Precipitation compared to landslide density.

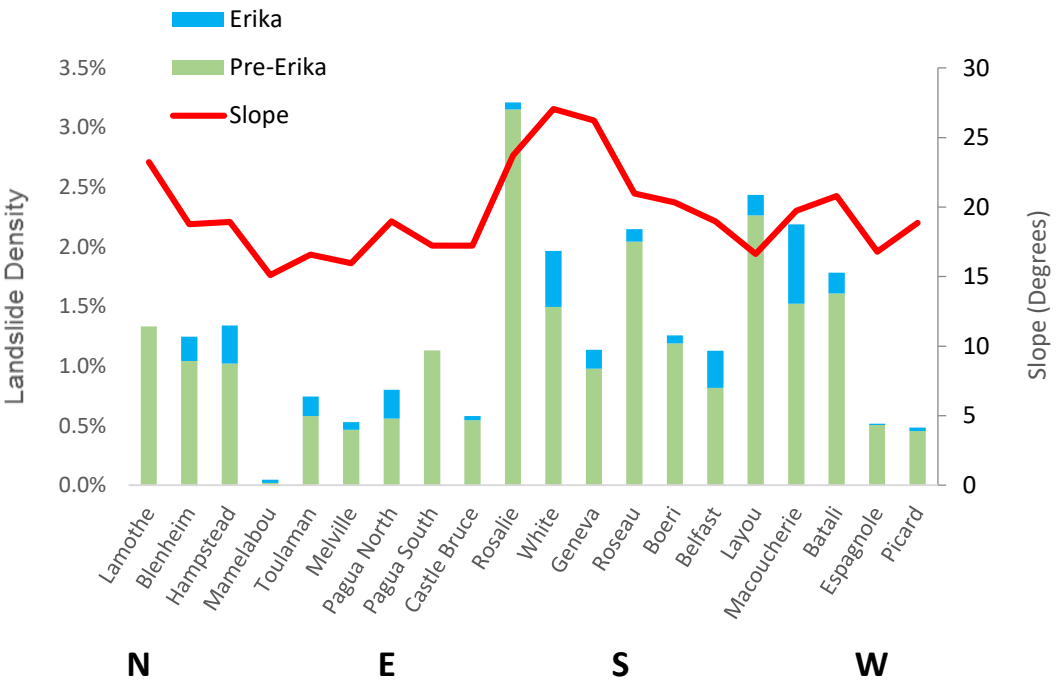

Figure 17. Slope compared to landslide density

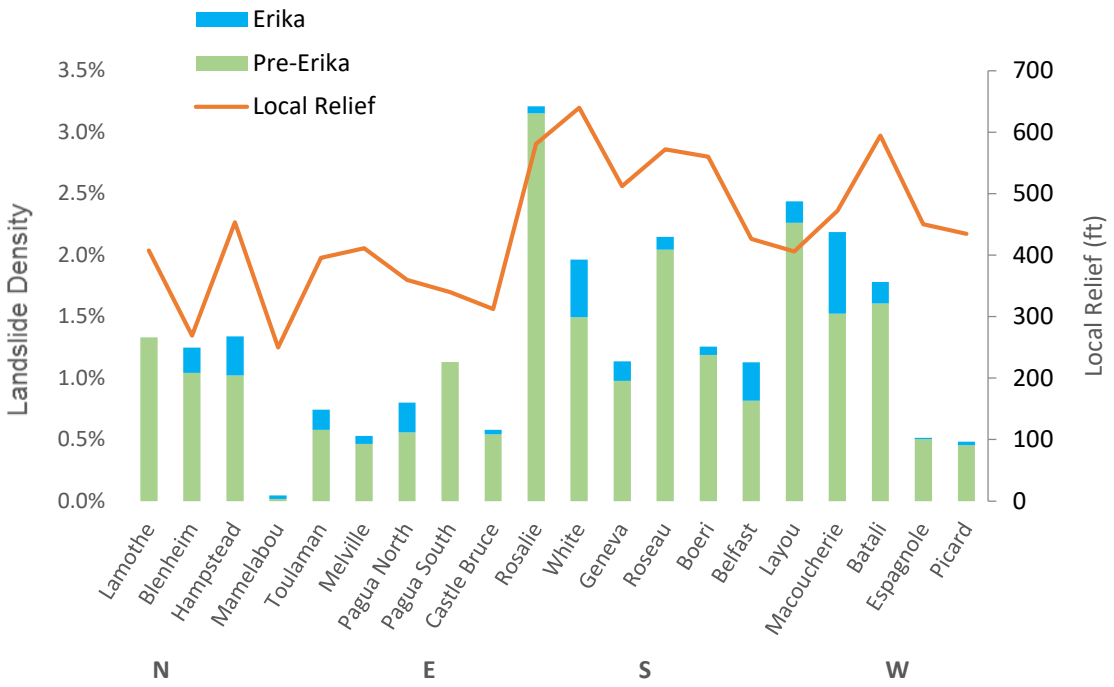

Figure 18. Local Relief compared to landslide density.

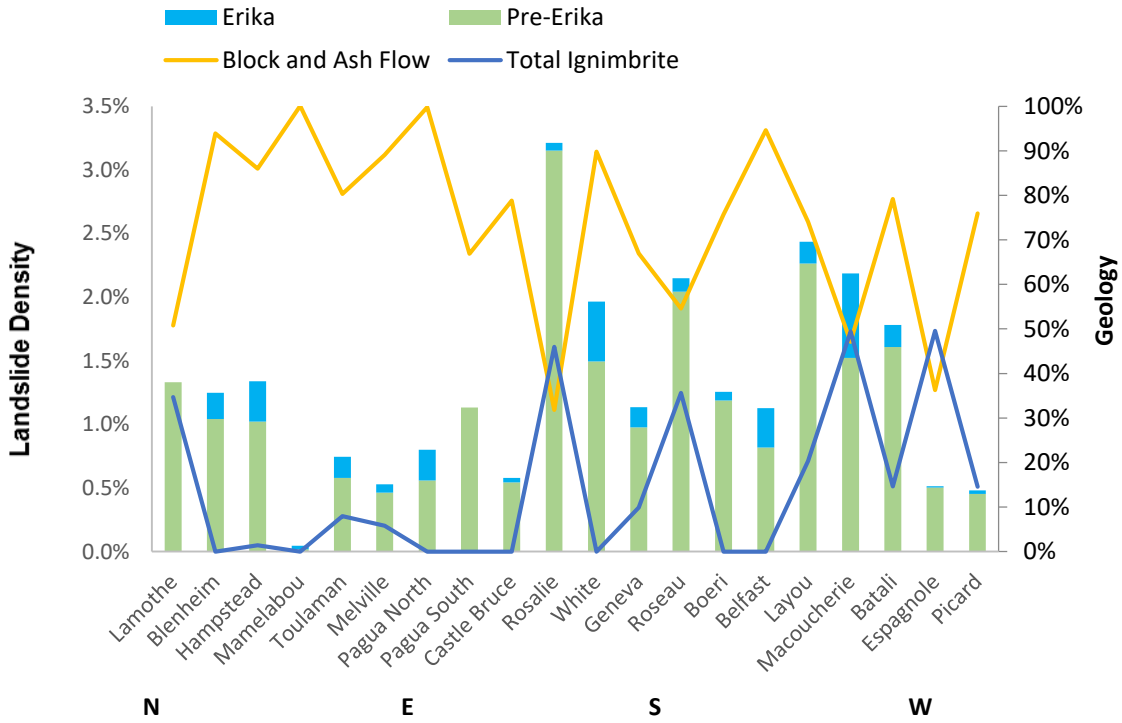

Figure 19. Major geologic units compared to landslide density.

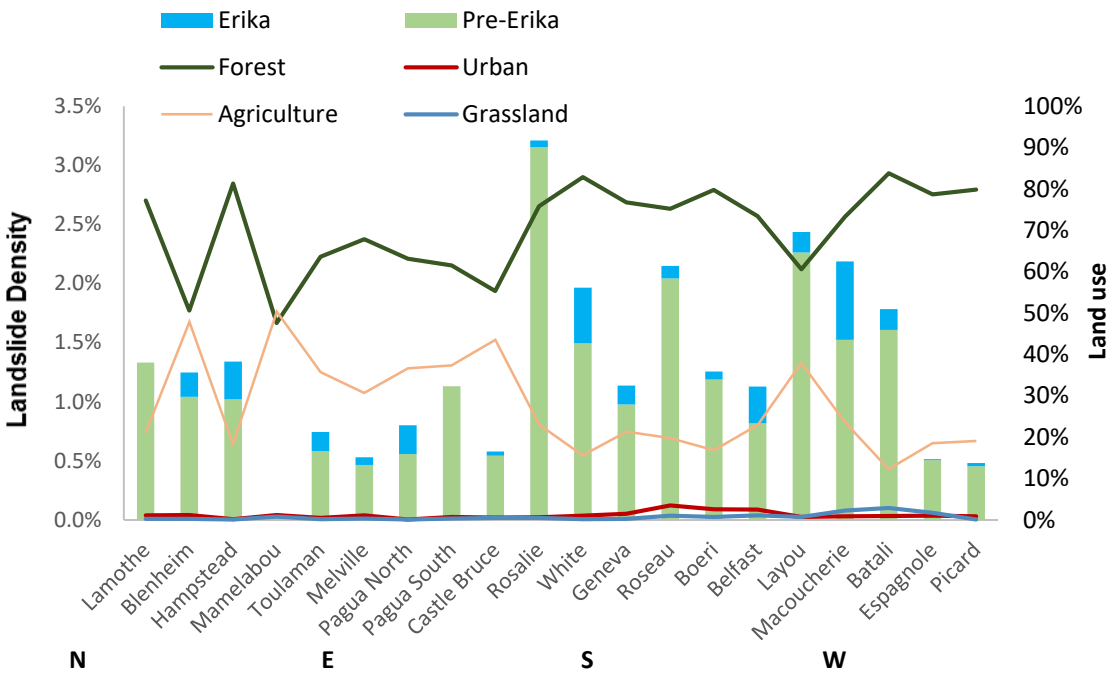

Figure 20. Major land use categories compared to landslide density.

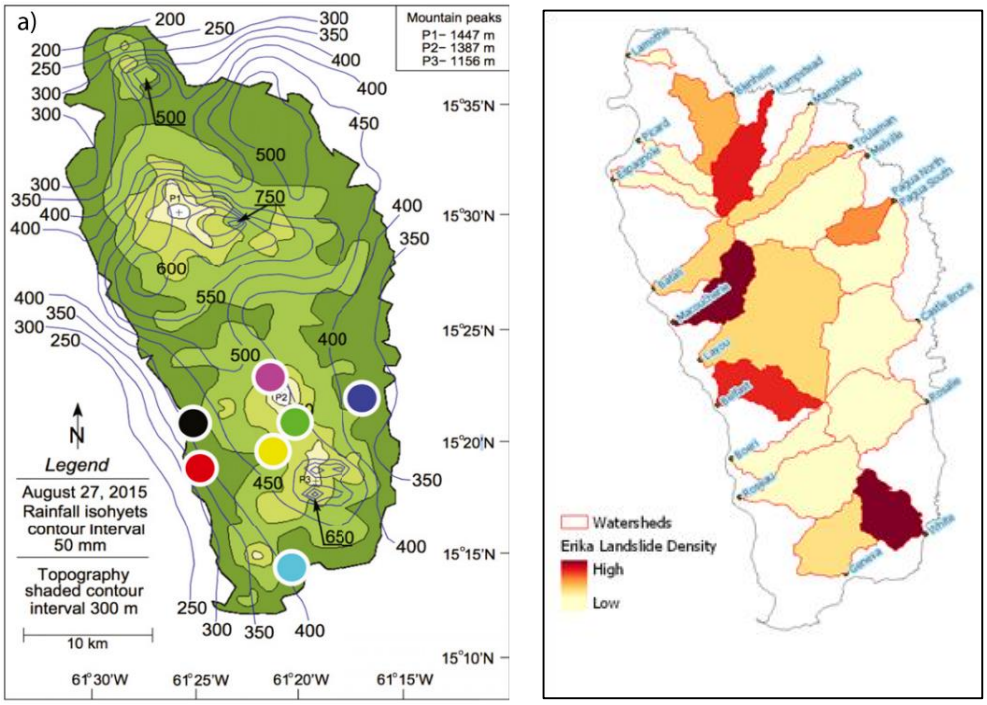

Figure 21. a) Isohyetal map of 24hr period during tropical storm Erika (Nugent and Rios-Berrios, 2017). Data is sourced from the Meteo-France Guadeloupe radar and a set of seven rain gauges. Colored dots are rain gauge locations. b) Landslide Density induced by Tropical Storm Erika.

Appendix A

River Name	GPS coordinates	DM	Date Sampled	Description
Geneva	15.24772, -61.31054	1	June 15th, 2017 @ 2:00PM	Sieved upstream and downstream of bridge 5-10% quartz Sub-rounded / sub-angular
Lamothe	15.62056, -61.46224	2	June 17th, 2017 @ 12:49PM	Lots of large boulders breaking up flow of stream and creating rapid features Average cobbles range from approximately 10-30cm Natural veg upstream and down Cement retention walls in place Sample downstream from bridge
Blenheim	15.59186, -61.39053	3	June 17th, 2017 @ 4:10PM	Low quartz% Lots of natural vegetation upstream Lots of large woody debris in channel Cobble deltas, ranging from 2-60cm Downstream streambed has much finer material Cement retention walls in place downstream
Hampstead	15.593264, -61.364223	4	June 17th, 2017 @ 5:12PM	People swimming and a car is parked in this river. Starts shallow but appears to get waist deep Decent amount of woody debris on fast flowing rapids slightly downstream of sampling location Vegetated, almost vertical wall on cutbank downstream Low quartz percentage Sampling just downstream (almost under) the bridge/overpass
Picard	15.559168, -61.45661	5	June 18th, 2017 @ 9:45AM	Average grain sizes ranging from ~2-10cm Retention wall on cutbank side, with undercutting on an almost vertical face Lots of large boulders (0.5m-1.5m) throughout channel Lots of fish, snails, crabs and lizards in and around channel and banks Right next to a grocery store and other houses/buildings Low quartz content Maybe 20M channel width, avg depth (ankle level) 10-20cm, up to 30 cm in depth Fast moving water
Espagnole	15.53322, -61.47484	6	June 18th, 2017 @10:56AM	Massive root ball, 2-3m wide, in the middle of stream Steam width <10m wide, fast moving water Root ball channelizing the stream= depth up 2m Predominantly gravelly banks,with a good amount of large cobbles (>10cm) Cobble bank downstream that becomes more narrow Lots of life in this water (crabs,minnows,etc) Upstream there are two bridges, one slumping into the water

Batali	15.45421, -61.44586	7	June 18th, 2017 @ 12:51PM	Lots of large woody debris in flow Mudbanks, relatively shallow slopes to banks, not a lot of veg on banks Streambed composed entirely of cobbles, fairly consistent size ~10-15cm Widest portion maybe 9-10m across, narrowest 1.5-2.0m across Average depth about ankle high, 5-15cm Branched upstream Single channelized downstream flow Lots of quartz
Macoucherie	15.42808, -61.432414	8	June 18th, 2017 @ 1:50 PM	Small cobble point bar ~5-15cm Cobble streambed, larger sizes than on pt-bar (25-30cm) River width @ sample location: 10m Slightly narrower upstream Slightly wider downstream (~15m) Lots of vegetation upstream Deep thalweg, ~55cm,fairly fast moving water 20% quartz Large, 1m high boulders on cutbank
Layou	15.40155, -61.41448	9	June 18th, 2017 @ 2:50PM	Large floodplain area with boulders up to 2m diameter Most are about 0.5m Cobbles, sand and a large dead tree (1.5m diameter) Cobble streambed, rounded/sub-rounded Most <25cm, occasional boulders Sampled upstream of dredging operations Channel ~40M wide at sample point, <0.5m deep except for deepest part (0.75-1.0m) Cut-bank has thick veg (bamboo and shrubs) 10% quartz
Belfast	15.36774, -61.40065	10	June 18th, 2017 @4:15PM	20m wide at sample point (upstream of bridge) rounded/sub-rounded cobble bed (25-30cm) with some boulders (in addition to cobbles & sand) 1m diameter boulders along bank Trees and shrubs on both banks Point bar is just upstream Fairly shallow (<0.5m) except for deepest point which looks to be about 1m deep fast-moving
Mamelabou	15.58527, -61.33514	11	June 19th, 2017 @ 9:40AM	Muddy banks Undercutting tree roots on both banks Wider upstream, narrows near sampling location before widening again downstream Narrowest point ~6M, Widest ~20M Creek flowing into stream a littlew ays downstream Large boulders downstream Low quartz %

Toulaman	15.55458, -61.30768	12	June 19th, 2017 @ 10:20AM	Huge boulders and cobbles on sandy delta that splits river in two Construction of wall on south bank Veg on north (natural) bank upstream, human activity on opposite bank Veg on both sides downstream South stream water depth much shallower and slower moving ~10cm on avg Appears to be much deeper and faster on north stream Narrower upstream After the two segmented portions rejoin total width maybe 20m
Melville	15.54690, -61.29571	13	June 19th, 2017 @ 11:03AM	Next to an airport People living and bathing on river (downstream of sampling location) Large boulders on opposite side (cutbank) Cobble point-bar with avg size ~2-15cm Looks to be about thigh deep on Cole at deepest part Not very wide, maybe 15m? 10-15% quartz Upstream: water is fast moving and both banks vegetated Coarse sand in-between cobbles and gravel on banks
Pagua North	15.51696, -61.27666	14	June 19th, 2017 @ 11:50AM	Two bridges near sampling location, one specifically for foot traffic Cows can be heard and seen around the location Lots of veg on both sides, up & downstream Large andesitic rocks w/dark (hornblende?) lithics present Fast moving, fairly shallow water 5% quartz
Pagua South	15.51539, -61.27788	15	June 19th, 2017 @ 1:03PM	Large boulders on opposite bank Mainly small cobbles, couple cm to like 20 ish on bank Fairly shallow near bank, deepest probably 80cm @ thalweg Veg upstream, retention wall downstream on far bank 20-30m wide Giant boulders in streambed
Castle Bruce	15.42808, -61.26051	16	June 19th, 2017 @ 3:00PM	Fairly deep water Cows on SE bank Very few cobbles on current bank/river bed but up and downstream there are cobble banks
White	15.27627, -61.25559	17	June 19th, 2017 @ 4:30PM	Bridge, deltas and cobbles Huge boulders, car sized and large tree around and under the bridge Sulfur covered rocks on top of mound of large cobbles Clearly remnants of Valley of Desolation Sulfur smell, fast moving water, looks to get pretty deep 15-20% quartz Exposed slope on opposite bank, maybe 30m high. Huge cobbles and boulders integrated in bank Downstream a bit, maybe 100m? Drains to ocean Channel width of about 20m, Fairly forested upstream Sub-rounded to rounded cobbles, <20cm

Rosalie	15.37234, -61.25467	18	June 19th, 2017 @ 5:43PM	Bridge a little upstream of where fine-grain sampled but downstream of where 250-850 gathered Large cobble delta slightly downstream of fine-grained sampling Large boulders on either bank Downstream to ocean, grasslands upstream 50m across at bridge Doesn't appear to be very deep Fast moving water ~10% quartz
Boeri	15.33101, -61.39152	19	June 21st, 2017 @ 8:39AM	No notes
Roseau	15.30247, -61.38582	20	June 21st, 2017 @ 10:00 AM	Two large bridges downstream of sampling banks heavily vegetated large cobbles boulders up to 0.5 m In Roseau city, densely populated area